PHILOSOPHICAL TRANSACTIONS OF THE ROYAL SOCIETY A MATHEMATICAL, PHYSICAL & ENGINEERING SCIENCES

The Aromatization and Isomerization of Hydrocarbons and the Thermal and Subsidence History of the Nova Scotia Margin [and Discussion]

A. S. Mackenzie, C. Beaumont, R. Boutilier, J. Rullkotter, S. A. F. Murrell, R. Mason, G. Eglinton and D. P. McKenzie

Phil. Trans. R. Soc. Lond. A 1985 **315**, 203-232
doi: 10.1098/rsta.1985.0037

Phil. Trans. R. Soc. Lond. A **315**, 203–232 (1985) [203]
Printed in Great Britain

The aromatization and isomerization of hydrocarbons and the thermal and subsidence history of the Nova Scotia margin

By A. S. Mackenzie[1]†, C. Beaumont[2], R. Boutilier[2] and J. Rullkötter[1]

[1] *Institut fur Chemie* 5: *Erdöl und organische Geochemie KFA-Jülich, Postfach* 1913, *D*-5170, *Jülich* 1, *West Germany*

[2] *Oceanography Department, Dalhousie University, Halifax, Nova Scotia B*3*H* 4*J*1, *Canada*

The temperature and burial histories of the sediments deposited on the continental margin off Nova Scotia have been modelled. A good match between predicted and observed present-day bottom-hole temperatures is only achieved when the thermal conductivities of sediments are derived from laboratory measurements of representative samples; values commonly quoted in the literature predict too low a geothermal gradient.

The temperature history is used to predict the extents of geochemical reactions involving steroid hydrocarbons together with previously derived reaction constants. The reaction extents were measured on 33 samples. In general, agreement between observations and predictions is good. The reactions in some samples, however, appear to have progressed anomalously far for their depths. This is thought to be the result of impregnation of these sediments with oil, which has migrated from depth.

The good general agreement between model predictions and observations encourages extrapolation of the model to areas of no sample control, and the reconstruction of the temperature and burial history of the margin. Tentative reconstruction of oil generation from the principal oil source rock of the region may also be attempted. The top of the oil-generation zone currently lies 4 km below the shallow regions of the continental shelf. Model predictions suggest that the Verrill Canyon formation and its equivalents are mature but that younger sediments are not. Maturation of deeper regions of the Verrill Canyon started in the Early Cretaceous, but significant volumes of sediment only entered the oil-generation zone during the Tertiary.

Introduction

Numerical modelling of the burial and thermal histories of sediments is used increasingly to predict the timing and location of petroleum generation in sedimentary basins (see, for example, Royden *et al.* 1980; Turcotte & McAdoo 1979; Turcotte & Angevine 1982). Although these models form a basis for reaching decisions concerned with the exploration for petroleum, few reliable and independent checks on the validity of the model predictions exist. The most important calibrants are present-day corrected bottom-hole temperatures; but these offer little control in areas where there are gaps in the sedimentary record and uplift and erosion of some consequence may have taken place.

Despite these uncertainties, a large number of poorly calibrated models for petroleum generation now exist. Such models invariably also suffer from an inadequate appreciation of the temperature-dependent reactions which convert the organic remains of dead organisms into

† Present address: BP Research Centre, Chertsey Road, Sunbury-on-Thames, Middlesex TW16 7LN, U.K.

petroleum. An initial attempt to overcome both these difficulties involves the study of organic chemical reactions that affect the organic compounds derived from the dead organisms deposited with the sediments during diagenesis (Mackenzie *et al.* 1982). The extents to which these reactions have occurred can be monitored by chemical analysis of sediments. Such measurements offer a means to quantify the integrated temperature history of their host sediment and increase the understanding of the reactions that affect sedimentary organic matter; they provide clues about the types of reactions related to petroleum generation and hence the temperature dependence of this process.

Before these reactions may be applied to the understanding of complex thermal history, their temperature dependence must be calculated. Laboratory studies (Abbott *et al.* this symposium) may help, but the major difference between laboratory and geological reaction times dictates that simple extrapolation of laboratory results would be unwise. The most promising approach to this problem is to calculate the temperature dependence of selected reactions by comparing numerical models for a number of sedimentary basins having simple burial histories with observations of reaction extents measured on sediments from these basins. By simple burial histories we imply no uplift, so that the present depth is the maximum depth. Mackenzie & McKenzie (1983) have already started this calibration by studying two basins with simple, but different, burial histories. This paper attempts three things with the relatively straightforward sedimentary sequence off Nova Scotia: further calibration of the temperature dependence of two chosen reactions, taking Mackenzie and McKenzie's work as a reference; further validation and examination of the previously reported numerical model of the burial and thermal histories of the sediments (Beaumont *et al.* 1982*a*); and tentative extrapolation of the results to the timing and location of petroleum generation.

Review of stretching models for continental margins

The extension model for the formation of rifted continental margins, also known as passive or Atlantic-type margins, proposed by McKenzie (1978) has been developed to describe both the subsidence of the lithosphere at a point (see, for example, Keen 1979; Royden *et al.* 1980; Royden & Keen 1980; Sclater & Christie 1980; Foucher *et al.* 1982; Jarvis & McKenzie 1980; McKenzie 1981) and complete cross sections of margins in which loading by sediments and water are supported by flexure of the lithosphere (Beaumont *et al.* 1982*a*; Steckler 1981; Sawyer *et al.* 1982; Sawyer *et al.* 1983). The model used by Beaumont *et al.* is reviewed here because it forms the basis of our present work.

In the uniform extension model (McKenzie 1978), the rifting phase of margin formation was described kinematically by the parameter $\beta(x)$, the amount of stretching of the lithosphere as a function of position. That the lower regions of the lithosphere, which have higher homologous temperatures than the crust, will extend by ductile flow as opposed to brittle failure and consequently by different amounts can be included by adding a second parameter, $\delta(x)$, describing extension in the ductile region (Royden & Keen 1980). Where $\beta(x) \neq \delta(x)$, the brittle and ductile regions are separated by a detachment surface (depth d) at which listric normal faults, thought to be diagnostic of stretching (Bally *et al.* 1981; Bally 1982; Montadert *et al.* 1979) are thought to sole out. (This depth-dependent stretching model gave the best results for the Nova Scotian margin (Beaumont *et al.* 1982*a*) and is used again in this work.)

An isostatic balance calculation between the unextended pre-rift and extended post-rift states

(Royden & Keen 1980; Beaumont *et al.* 1982*a*) shows that the initial subsidence on extension is a function of the densities, thicknesses and thermal properties of the component parts of the lithosphere.

The post-extensional phase of tectonic subsidence is largely controlled by the thermal evolution of the lithosphere. Thermal disequilibrium exists within the lithosphere following rapid extension, because material which has moved upward as well as laterally during extension advects heat and asthenosphere at or near the melting temperature flows into space formerly occupied by relatively cooler lithosphere. Thermal equilibrium is restored by the conductive cooling of the lithosphere, with a time constant proportional to the square of the thickness of the thermally stable lithosphere. Cooling is accompanied by thermal contraction and subsidence. In the absence of amplification by loads, the thermal contraction subsidence, which together with the initial subsidence comprises the tectonic subsidence, is related in a simple way to the change in average temperature of the lithosphere during cooling (Beaumont *et al.* 1982*a*). The simple analytical expressions for subsidence no longer apply when the lithosphere is loaded and insulated by sediment. McKenzie (1981) showed one way of solving this problem, while others have used finite-difference or finite-element numerical models (Royden & Keen 1980; Beaumont *et al.* 1982*a*; de Bremaecker 1983; Issler 1984*b*).

Beaumont *et al.* (1982*a*) used a coupled thermo-mechanical model for the post-rift evolution of margins, in which thermal evolution of a margin cross section is based on interpolations between one-dimensional finite-difference solutions for the diffusive cooling and thickening of a self-contracting sediment-blanketed lithosphere, as a function of changing $\beta(x)$ and $\delta(x)$ with position. A coupled mechanical finite-element model calculates the isostatic response to loading. The mechanical model is necessary because the lithosphere, the Earth's thermal boundary layer, behaves as a mechanically strong region that can undergo flexure during isostatic adjustment to surface loads, in a manner that is primarily determined by its thickness and internal temperature distribution (Bodine *et al.* 1981; Watts *et al.* 1982; Courtney & Beaumont 1983). Rifted margins have variable flexural rigidity, a measure of the flexural strength. Beneath the continental region, where there is little or no extension, the lithosphere remains strong, whereas in highly stretched regions, thinning of the lithosphere and fracture of the brittle part of the crust both contribute to making the lithosphere mechanically weak. Thinned regions cool down as they age, like oceanic lithosphere (Parsons & Sclater 1977) and the mechanical strength returns. The finite-element method is an appropriate way to calculate flexure of a lithosphere that has properties which vary in time and in space.

We assume that regions of the lithosphere where the temperature is less than a certain value, T_R, remain elastic and undergo flexure, whereas hotter regions flow rapidly in a viscous manner to relax stress and can therefore be regarded as a fluid that contributes only basal buoyancy forces to the overlying flexed elastic region. This division into two regions is justified for a lithosphere in which viscosity is temperature dependent (Courtney & Beaumont 1983; Beaumont *et al.* 1984). Regions with high or low homologous temperature relax stress rapidly and appear inviscid or do not relax stress and act elastically respectively, on the timescales of processes recorded in the stratigraphy of continental margins. There is a viscoelastic region between the effectively elastic and inviscid regions that can be ignored while the margin is cooling. Choice of T_R cannot be made *a priori*, because it depends on the mineralogy and activation energy for viscous flow parameters, which are not known precisely.

It is now evident why a coupled thermo-mechanical model is used. The thermal evolution

determines the tectonic subsidence and the depth of the relaxation isotherm. The mechanical model then determines the flexural response to loads which fill and amplify tectonic subsidence. Feedback from thermal blanketing and erosion modify cooling, thermal contraction and subsidence.

The properties of the model sediments are discussed in detail by Beaumont *et al.* (1982*a*). Sediments undergo exponentially increasing compaction by expulsion of water. Each major lithology is assigned a surface porosity and its decay depth is determined from sonic and density logs of wells. Two component lithologies are also allowed. The thermal properties of the sediments are determined by the conductivity of their matrix constituents and their porosity. Radiogenic heat production in the sediments and crust can also be included. The relation of these properties to temperature is discussed later.

The computational methods used in the coupled thermo-mechanical model may be summarized as follows. The required input variables are the variation in $\beta(x)$ and $\delta(x)$, the value of T_R, the values of the thermal, mechanical and sedimentological parameters and the sediment budget. Calculations are done by taking model time steps of *ca.* 10–20 Ma. The procedure is as follows.

(i) At $t = 0$, extension occurs, resulting in the initial subsidence as predicted by local isostatic adjustment. This depression is then filled with a combination of sediment and water to simulate loading of the continental margin just after formation. Isostatic adjustment to this load is calculated by using the mechanical model described above.

(ii) A time interval Δt elapses during which the lithosphere cools and subsides as predicted by the thermal model; the position of the isotherm T_R also changes and a further load of water and sediment accumulates. Isostatic adjustment is again calculated by the mechanical model, adjusted for the new depth of T_R.

(iii) This process is continued over the number of time steps necessary to simulate the evolution of the margin. After each time step, the depths to the sea floor and to the basement, the position of the Moho discontinuity, the temperature distribution and the gravity anomaly across the margin are computed.

Results of a thermo–mechanical model of the Nova Scotian margin

A cross section of the Nova Scotian continental margin along seismic multichannel line 108 (figure 1) was modelled by Beaumont *et al.* (1982*a*), who discuss the primary sources of data shown on the cross section (figure 2). The interpreted cross section, in particular the stratigraphic data from wells, was compared with the predictions of a thermo-mechanical model in which the rifting models, T_R, $\beta(x)$ and $\delta(x)$ were varied across the margin to achieve the best fit. The seismically determined crustal thickness was used to estimate $\beta(x)$ on the assumption that the crust was uniformly 35 km thick, like that adjacent to Nova Scotia, before stretching. Small variations from these estimates were allowed to achieve the desired stratigraphy when sediments in amounts equal to those observed, but in a decompacted form, were added at each time step.

A value $T_R = 250$ °C was chosen by comparing observed and predicted gravity anomalies, although a more deeply buried elastic core of equivalent thickness is equally acceptable. $\delta(x)$ was varied to minimize paleobathymetry, in those areas thought to have been the continental shelf, and to cause transient initial uplifts to delay sedimentation where necessary. We regard

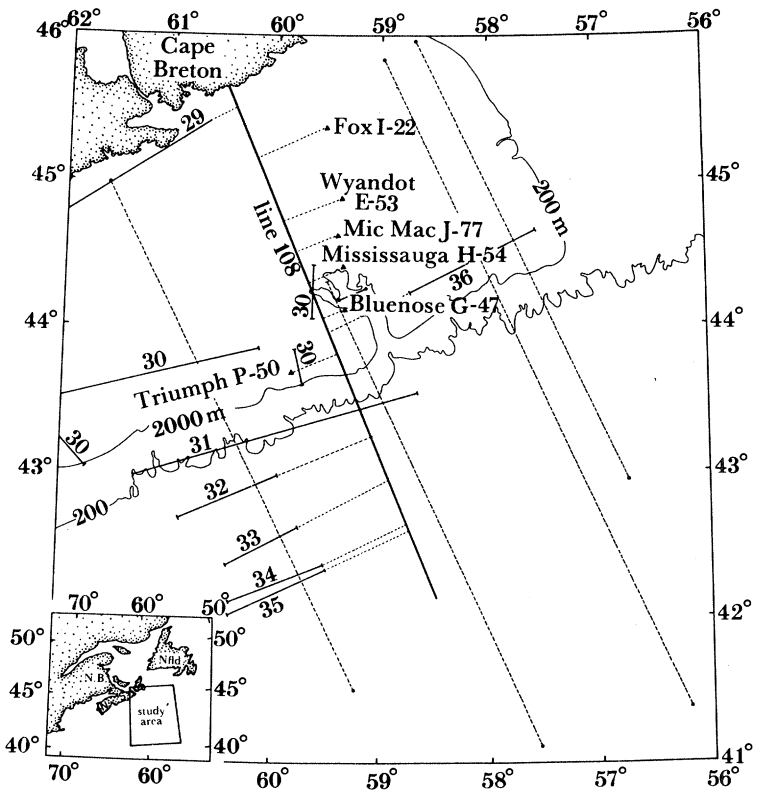

FIGURE 1. Sources of structural data used in the Nova Scotian study. The heavy solid line (line 108) is the cross section (shown in figure 2). The triangles show deep exploratory wells. The broken lines are the tracks along which free-air gravity anomalies have been measured. Solid lines show the position of deep crustal seismic refraction lines. The well and refraction data have been projected (fine broken lines) on to line 108. (Beaumont *et al.* 1982*a*.)

$\delta(x)$ to be poorly determined as a result of the interpretive nature of the basin stratigraphy near its base.

Figure 3 shows several stages in the evolution of the model stratigraphy used in this paper. The model has a slightly different $\beta(x)$ and $\delta(x)$ from that of Beaumont *et al.* (1982*a*). Improved values were chosen to represent the subsidence at some of the well locations, in particular Wyandot and Mic Mac.

The model predicts unrealistic paleobathymetry during the Jurassic, probably reflecting errors in the model sediment budget in the poorly known deep regions of the basin. The paleobathymetry becomes more realistic by the end of the Jurassic, 144 Ma ago. Minor truncation of the sediments occurs during the later stages of the model's evolution, indicating that locally there is insufficient tectonic and flexural subsidence to accommodate the interpreted sediment distribution (figure 2).

The subsidence history of the model margin is insensitive to realistic variations in the thermal properties of the sediment. The overall blanketing effect of the sediments does, however, reduce the subsidence in the deepest parts of the basin by *ca.* 1 km, by comparison with a basin in which the sediments were assumed to have infinite thermal conductivity.

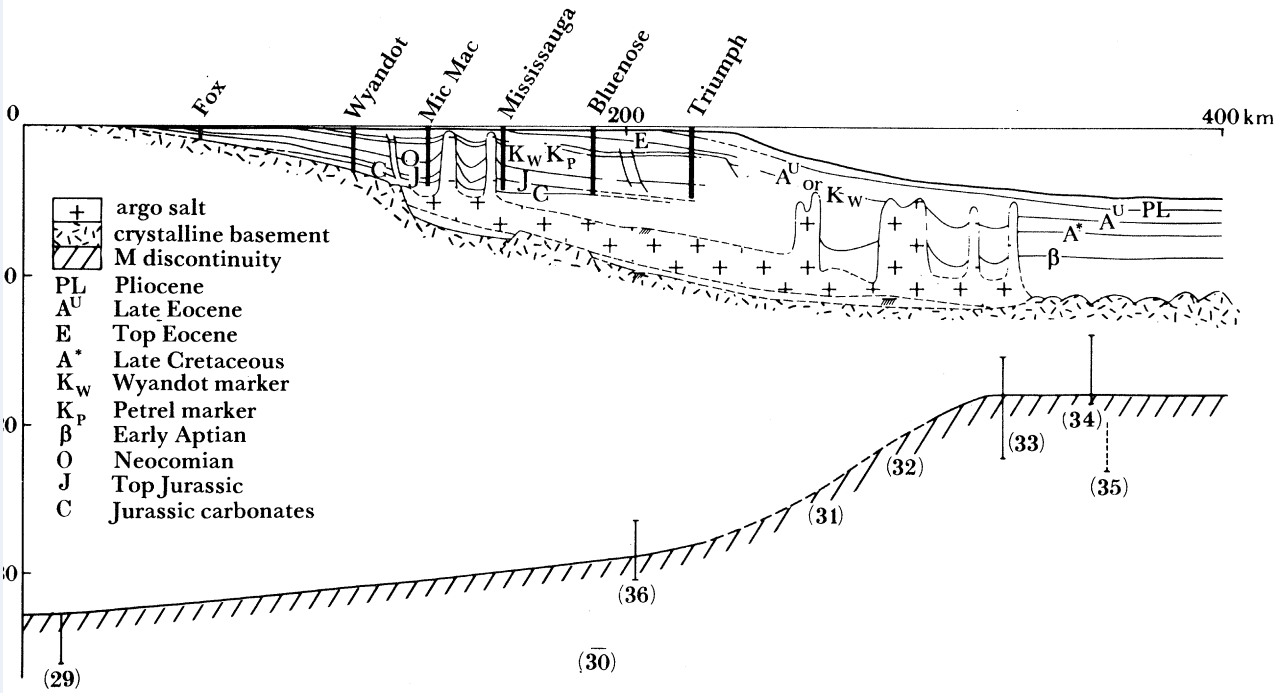

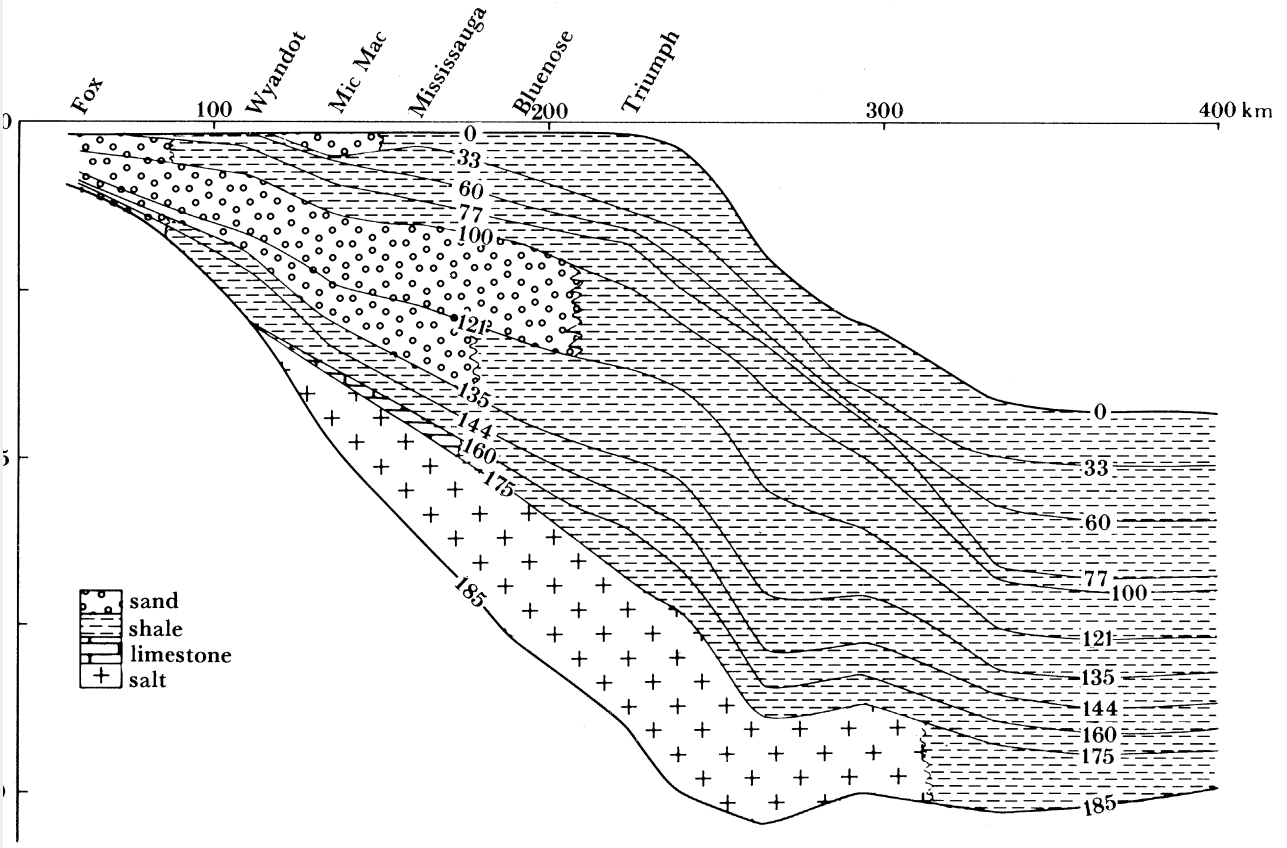

FIGURE 2. Generalized and interpreted chrono- and litho-stratigraphy of the Scotian Basin along the section of figure 1. This interpretation has a chronostratigraphy that was also used in the theoretical models. The section has been restored to remove the effects of diapirism and the lithology simplified to include the four components shown. In the cross section only the dominant sediment type in an area for a given time interval is shown; however, the calculations allowed for mixtures of two components and such mixtures were used. This is the section that was decompacted and used as the sediment budget for the theoretical models.

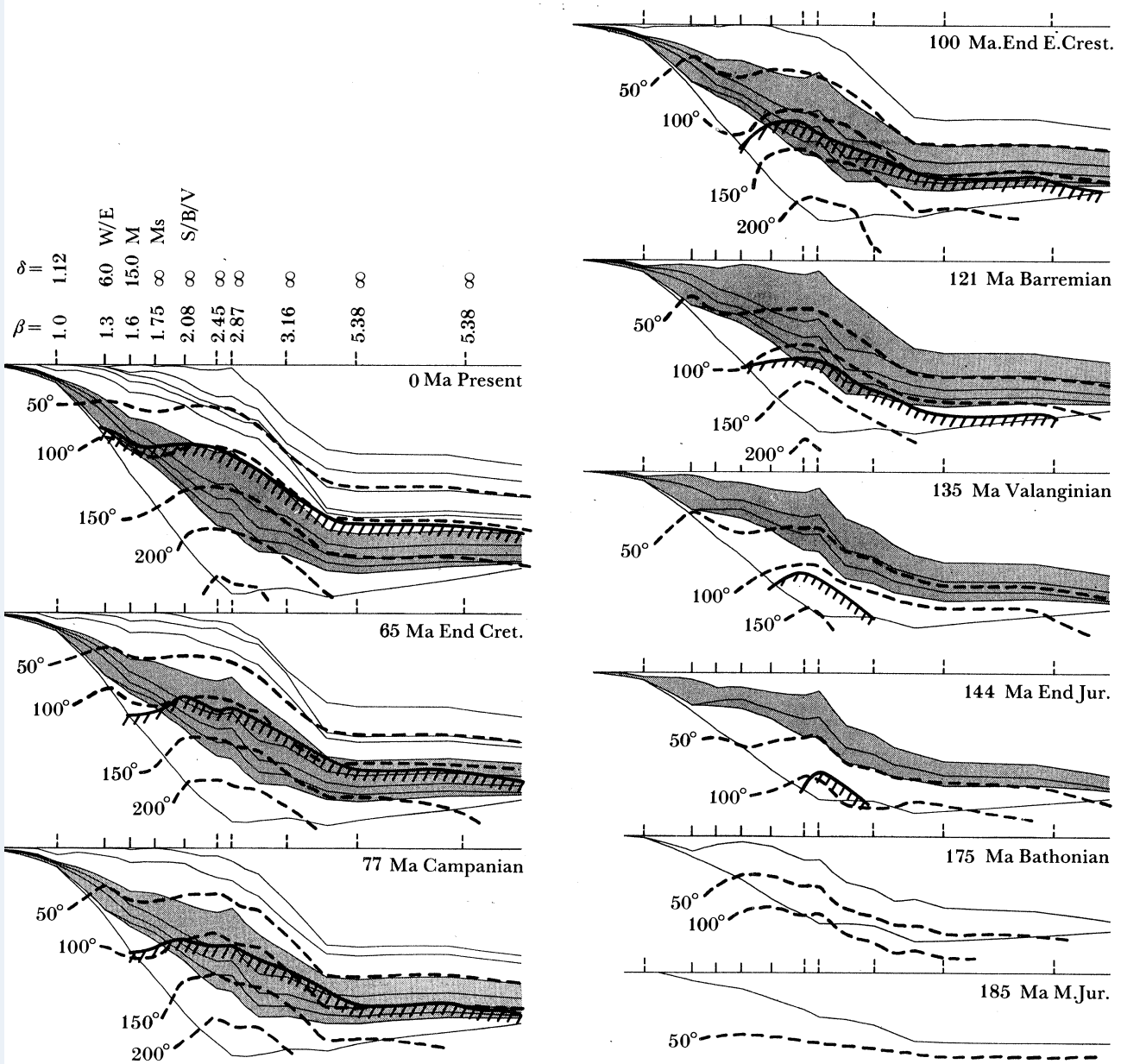

FIGURE 3. Diagrams showing the evolution of the Nova Scotian cross section as predicted by thermo–mechanical model B. Solid lines are the chronostratigraphic horizons corresponding to those shown in figure 2. Bold broken lines show the positions of isotherms and the bold underscored line is the predicted location of the top of the oil-generation zone. The shaded area shows the Verrill Canyon formation and its equivalents. The distribution of the δ and β stretching factors and the position of the wells are given. W, Wyandot; E, Erie; M, Mic Mac; Ms, Mississauga; S, Sable Island; B, Bluenose; V, Venture.

THERMAL HISTORY AND MATURATION OF MARGIN SEDIMENTS

Previous sections have focused on the structural, subsidence and sedimentary history of continental margins. We now turn our attention to the thermal history of the sediments. Three aspects contribute to the temperature, (i) lithospheric cooling, which determines the basal heat flux into the sediments, (ii) the thermal properties of the sediments and in particular their thermal conductivity, which determines how good an insulator the blanketing sediment

becomes and (iii) heat production from radiogenic elements in the sediments and upper crust. We assume that heat is transferred mainly by conduction and that fluid convection or the flow of fluids expelled during compaction are not significant. This is not always true, as shown by Oxburgh & Andrews-Speed (1981), Hitchon (1984), Garven & Freeze (1984*a*, *b*) and Beaumont *et al.* (1985). The validity of the assumption for our present example is, however, confirmed by comparison of observations with model predictions.

The temperature history of sediments is potentially important because it may be possible to relate the temperature-dependent conversion of kerogen to oil and gas to the temperature history and hence predict if, when, and where oil and gas generation occurred in source areas for a potential petroleum trap. The ability to make these estimates within a sedimentary basin from sparse data (such as seismic stratigraphy, isolated wells and some knowledge of thermal conductivity of the sediments) would therefore assist in oil and gas exploration, particularly in frontier areas.

While it is generally agreed that the maturation of sedimentary organic matter is related to temperature, it is not clear that knowing the temperature history will enable us to predict sediment maturity. The first step in testing this hypothesis is to find a method of checking the accuracy of thermal history predictions. Once we are confident that we know past and present temperatures accurately, their relation to maturation can be established.

Present temperature–depth predictions can be compared with corrected bottom-hole temperatures, but past conditions cannot be retrieved because no suitable accurate geothermometer exists. The maturation indicators, of which vitrinite reflectance is the most commonly used, do not provide a quantitative measure of temperature history. This is partly because the reflectance scale is empirical and must be calibrated with presumed temperature histories and partly because vitrinite has a range of reflectance behaviour with temperature because of its compositional variability. Stable isotopes, conodont coloration, inorganic geochemical indicators and thermal alteration indices are no better. Any method that relies on phase equilibria is potentially suspect, because the very existence of an equilibrium for given P–T conditions depends on the availability of chemical species that may be limiting in the reactions.

A different approach is to use the kinetics of specific reactions. Thermally activated reactions in organic molecules may provide constraints on temperature history against which theoretical predictions can be tested. In principle, the kinetic parameters of a reaction, the activation energy and frequency factor, are measured. The degree to which the reaction has progressed in the sediment column is then predicted by integrating the reaction equations with the use of the model thermal history. The amount of reaction in samples is then measured for comparison. If we are confident that we know kinetic parameters with sufficient accuracy, the comparison, when applied to a suite of samples, allows the model thermal history to be accepted or rejected. In this section, we discuss the application of this technique by using aromatization and isomerization reactions of specific hydrocarbons as our constraint on model temperature histories.

The aromatization and isomerization (a.–i.) reactions

In recent years, the understanding of the fate of organic constituents from dead organisms which are incorporated in sediments during deposition has increased (Ourisson *et al.* 1979; Mackenzie *et al.* 1982). The initial reactions are complex and microbial processes are as important as the effect of the temperature rise associated with burial (Brassell *et al.* this

symposium). The subsequent reactions of the mainly saturated hydrocarbons (alkanes) or aromatic hydrocarbons remaining at temperatures greater than 50 °C are less complex and are mainly a response to increasing temperature. The high structural specificity of natural product compounds, which is determined by enzymatic biosynthesis and the function of the molecule in the host organism, is inherited by the hydrocarbons. Thus, both the reactants and products of chemical reactions can be recognized, and their relative concentrations used as a measure of the extent of thermal maturation of the host sediment (Mackenzie & Maxwell 1981).

Three reactions have been studied in some detail (figure 4). Figure 4*a* illustrates that sterols, common constituents of the cell membranes of algae and higher plants, are converted in part to steranes during early diagenesis (Rhead *et al.* 1971; Dastillung & Albrecht 1977). This conversion involves the loss of the hydroxyl group at C-3 and the double bond connecting C-5 to C-6. The basic stereochemistry (three-dimensional shape) of the sterane molecule is the same as that of the precursory sterol, namely 8β*H*, 9α*H*, 10βCH_3, 13βCH_3, 14α*H*, 17α*H*, 20(*R*), where α implies that the bond to the named part of the molecule (*H* or CH_3) points into the page when the molecule is drawn in the orientation shown in figure 4*a*; β implies that the bond points out of the page. The α stereochemistry is represented by a broken line when the bond is between two carbon atoms and by an open circle for carbon–hydrogen bonds; the β stereochemistry is shown as a solid triangle and a dot respectively.

When the carbon atom of interest is not part of a ring system (for example, C-20 in figure 4*a*), its stereochemistry is defined as (*R*) or (*S*) (Gunstone 1974). Two variants always exist when the substituents attached to the carbon atom are all different. Natural product sterols all have the 20(*R*) configuration and this is passed on to the steranes of immature sediments. The 20(*S*) isomer, where the methyl group attached to the C-20 points out of the page instead of into the page (figure 4*a*), is of similar stability to the 20(*R*) isomer. At elevated temperatures (*ca.* 65 °C), hydrogen is removed from C-20 by an unknown mechanism and the resulting intermediate can regain a hydrogen atom on either side of the molecule. Thus, the equilibrium of $20(S)/[20(R)+20(S)] = 0.54$ (Van Graas *et al.* 1982) is steadily approached between temperatures of 65 and 130 °C. This reaction type is called isomerization.

An analogous reaction is the isomerization of hopanes at C-22 (figure 4*b*). Hopanoids are common constituents of the cell membranes of bacteria (Ourisson *et al.* 1979), which convert partly to 17α*H*-, 21β*H*-hopanes during early diagenesis (figure 4*b*). The hopanoids of living organisms chiefly exist with the (*R*) stereochemistry at C-22; this stereopreference is inherited by the hopanes of immature sediments (**1** in figure 4*b*). Again, elevated temperatures cause hydrogen exchange at C-22 thereby converting 22(*R*) isomers into 22(*S*) isomers (**2** in figure 4*b*). The corresponding $22(S)/[22(R)+22(S)]$ value rises from 0 to about 0.60 with increasing maturity (Ensminger *et al.* 1974, 1977; Seifert & Moldowan 1980). In most of the Nova Scotian samples studied, this reaction had gone to completion and it is therefore not possible to use it to determine the thermal history of the host sediment. Although the results are presented in table 1, they are not discussed further.

The third reaction of interest involves aromatization. The monoaromatic steroid hydrocarbons (**1** in figure 4*c*) are formed during early diagenesis. At higher temperatures, further aromatization occurs; 7 hydrogens and 1 methyl substituent are lost to produce triaromatic steroid hydrocarbons (**2** in figure 4*c*). Unlike the isomerization reactions, the aromatization reaction has no significant backward reactions and almost all the monoaromatics appear to be converted to triaromatics with increasing thermal maturity.

Steroid hydrocarbons with 26–30 carbon atoms occur in most organic-rich sediments;

PHILOSOPHICAL TRANSACTIONS OF THE ROYAL SOCIETY A MATHEMATICAL, PHYSICAL & ENGINEERING SCIENCES

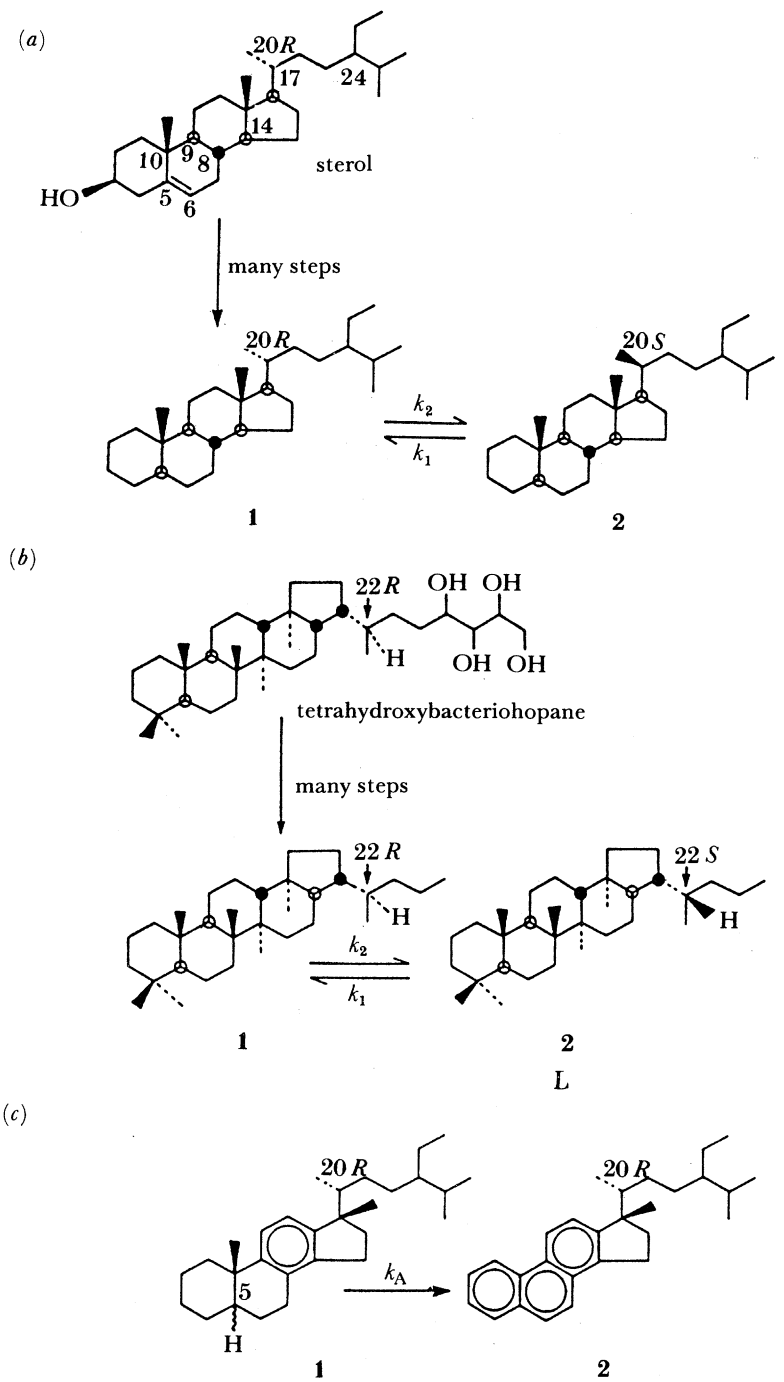

FIGURE 4. (*a*) Representations of the molecules of a sterol, found in living organisms and the two isomeric steroid hydrocarbons **1** and **2**, found in sediments, that are used to determine the extent of isomerization. The configuration at one chiral centre (C-24) is not indicated because the two isomers were not resolved by the g.c.–m.s. system we used. Of the **256** possible arrangements of the eight chiral centres shown, only two are present after early diagenesis. Hydrogen exchange then occurs at C-20 by removal and then reattachment of the hydrogen atom. (*b*) Representations of a hopanoid molecule found in living organisms (tetrahydroxybacteriohopane) and the two isomeric hopanes found in sediments which were used to determine the extent of isomerization, **1** and **2**. (*c*) **1** represents two monoaromatic steroid hydrocarbons, which are isomeric at C-5 (shown by the sinuous C–H bond), with the aromatic ring shown by an inscribed circle. With increasing temperature, hydrogen and a methyl group are lost to produce a triaromatic hydrocarbon, **2**. The reaction is assumed to be irreversible under geological conditions. As in 4*a*, the chiral centre at C-24 is not shown.

TABLE 1. SAMPLE MEASUREMENT RESULTS

sample[a] code no.	percentage organic carbon	reaction extents[b, c] sterane isomerization x	hopane isomerization y	steroid aromatization z	contains migrated oil
M13	0.9	0.48	0.57	0.88	—
M14	0.9	0.44	0.55	1.00	—
Ms15	0.8	0.32	0.50	0.43	*
Ms17	1.8	0.16	0.34	0.22	—
Ms18	1.4	0.48	0.56	0.85	—
Ms19	1.6	0.43	0.57	0.86	—
Ms20	1.0	0.51	0.66	0.75	—
Ms21	0.5	0.53	0.57	1.00	—
B22	0.7	0.15	0.30	0.13	—
B23	0.8	0.24	0.27	0.16	*
B24	0.8	0.32	0.50	0.16	*
B25	0.5	0.34	0.49	0.14	*
B26	2.4	0.19	0.47	0.16	—
B27	1.3	0.26	0.53	0.38	—
B30	7.0	0.43	0.58	0.62	—
B31	0.7	0.53	0.60	1.00	—
B32	0.6	0.40	0.53	0.83	—
E35	0.7	0.34	n.d.	0.60	*[d]
W37	0.05	0.37	0.57	0.51	—
S38	0.57	0.27	0.23	0.11	*
S39	1.88	0.12	n.d.	0.11	—
S40	0.20	0.35	0.57	0.40	—
S41	1.50	0.37	0.64	0.90	—
V44	1.5	0.48	0.65	0.81	*
V45	0.3	0.11	0.27	0.07	—
V46	0.5	0.36	0.51	0.31	*
V47	1.0	0.40	0.52	0.23	*
V48	1.0	0.25	0.32	0.19	—
V49	1.5	0.23	0.44	0.58	—
V50	1.0	0.41	0.55	0.70	—
V51	1.5	0.47	0.61	0.64	—
V52	1.3	0.58	0.64	1.00	—
V53	1.0	0.57	0.60	1.00	—

[a] M, Mic Mac; Ms, Mississauga; B, Bluenose; E, Erie; W, Wyandot; S, Sable Island; V, Venture.

[b] The error estimates are ± 0.04; see text for details.

[c] Ratios $= 2/[1+2]$

$x = (20(R) - C_{28}$ triaromatic steroid hydrocarbons$)/(20(R) - C_{28}$ triaromatic steroid hydrocarbons$) +$ $(20(R) - C_{29} - 5\alpha H + 5\beta H -$ monoaromatic steroid hydrocarbons$)$

$y = (20(S))-/(20(S))-+(20(R))-24$-ethyl $5\alpha H$, $14\alpha H$, $17\alpha H-$cholestane

$z = (22(S))-/22(S)-+(22(R))-17\alpha H$, $21\beta H-$bishomohopane.

[d] Values n.d. are not determined; components not present in sufficient quantity.

therefore, there are a large number of possible ratios of reactants to products which could be used to measure the progress of the reactions. We use the same ratios as Mackenzie & McKenzie (1983).

The degree of aromatization is measured by $x = B/(M+B)$, where M includes all four of the C_{29} monoaromatics with a $20(R)$ stereochemistry (those isomeric at C-5 ($5\alpha H$ and $5\beta H$) and at C-24 ($24(R)$ and $24(S)$); and B is both of the C_{28} triaromatics with a $20(R)$ stereochemistry (the isomers at C-24). The aromatization results in the loss of one carbon atom and the stereochemistry at C-5 (figure 4*c*).

The degree of sterane isomerization at C-20 is measured for C_{29} 5α*H*, 14α*H*, 17α*H* compounds (figure 4*a*) by the ratio $y = 20(S)/[20(R)+20(S)]$. In each case (20(*R*), 20(*S*)), the combined amount of the two compounds with a 20(*R*) or 20(*S*) stereochemistry is used. Each isomer is also isomeric at C-24 and both 24(*R*) and 24(*S*) isomers occur in sediments (figure 4*a*).

The degree of hopane isomerization of C-22 is measured for compounds with the most stable configuration at C-17 and C-21 (17α*H*, 21β*H*) (see figure 4*b* of Ensminger *et al.* 1974). The isomerization at C-22 occurs in all hopanes with more than 30 carbon atoms and C_{31}–C_{35} compounds commonly occur in sediments. We concentrate on the C_{32} species, the degree of aromatization of which is measured by $z = 22(S)/[22(R)+22(S)]$. Each measured isomer (22(*R*), 22(*S*)) represents a single component.

The details of the analytical techniques can be found in Mackenzie & McKenzie (1983) and Mackenzie *et al.* (1983) and references therein. The values of ratios *x*, *y*, and *z* are determined by analysing the total hydrocarbon fraction, extracted from the sedimentary rock sample, with gas chromatography–mass spectrometry (g.c.–m.s.). By increasing the resolution of the mass spectrometer, it is possible to determine the ratios in about one hour from a single analysis of an extract of a sedimentary rock (Mackenzie *et al.* 1983).

If the reactions are first order, the rate coefficients (*k*) can be calculated from the formulae given by Mackenzie & McKenzie (1983). The measured values of *x*, *y*, and *z*, the reaction time, *t*, and the ratio γ of the forward reaction rate coefficient, k_2, to the back reaction rate coefficient, k_1, are required. *k* varies with temperature according to the Arrhenius Law

$$k = A \exp(-E/RT), \tag{1}$$

where *A* is the frequency factor, *E* the activation energy, *R* the gas constant and *T* the absolute temperature. Mackenzie & McKenzie (1983) argued that, given the likely errors associated with their many assumptions, *A* and *E* may be regarded as constants. They estimated *A* and *E* for the different reactions in two ways. They first used analytical solutions of (1) for samples whose present and known temperatures are their maximum values. *t* was assumed to be the time spent within 15 °C of the maximum temperature because most of the reaction will have occurred in this interval (Hood *et al.* 1975). γ was estimated from samples where equilibrium appeared to have been attained and from published estimates of the differences of heats of formation of reactants and products (Van Graas *et al.* 1982). Estimates of *A* and *E* were found from the intercept and slope of a plot of $\ln k$ against $1/T$ (1). These estimates were further improved by using numerical solutions of the reaction equations in which the temperature histories of the analysed samples were predicted by the model of McKenzie (1981) of sedimentary basins formed by crustal stretching. Plots of one reaction extent against another for stretched basins of different ages were used to guide the adjustment of *E* and *A* for each reaction until the predicted and observed values were in broad agreement. Mackenzie & McKenzie (1983) have been able to fit the data from seven sedimentary basins formed by crustal stretching events of age −180 to −15 Ma with a single set of reaction constants. They also demonstrated that the assumption of first-order kinetics for the isomerization reactions is apparently valid. This assumption remains untested in nature in the case of the aromatization reaction, although G. D. Abbott *et al.* (this symposium) found the reaction to obey first-order kinetics when performed in the laboratory. The estimates of *E*, *A* and γ for each of the reactions are given in table 2.

PHILOSOPHICAL TRANSACTIONS OF THE ROYAL SOCIETY A MATHEMATICAL, PHYSICAL & ENGINEERING SCIENCES

TABLE 2. MACKENZIE & MCKENZIE (1983) ESTIMATES OF REACTION CONSTANTS

reaction	E/(kJ mol^{-1})	A/s^{-1}	γ
sterane isomerization at C-20	91	k_2 0.007 k_1 0.006	1.174
hopane isomerization at C-22	91	k_2 0.025 k_1 0.016	1.564
steroid hydrocarbon aromatization	200	k_2 1.8×10^{14}	∞

E = activation energy; A = frequency factor; k_1 = back reaction rate coefficient; k_2 = forward reaction rate coefficient; $\gamma = k_2/k_1$.

The implications of these values for reaction mechanisms and the effect of burial and heating rates of sedimentary sequences on the reaction rates are discussed by Mackenzie & McKenzie (1983).

COMPARISON OF SAMPLE RESULTS WITH THEORY

The isomerization and aromatization reactions have been examined in 55 samples from seven wells, or well groupings, in the Scotian Basin. We report here on the results of 33 samples; the remaining 22 did not contain the reactants and products in sufficient amounts, either because of the low overall organic matter content or because of high maturity. After the completion of the reactions, the remaining reactants and products are both converted by subsequent reactions to other, as yet, unidentified compounds (Mackenzie *et al.* 1985).

The wells (figure 5) are located close to multichannel line 108 and the section of the model discussed earlier. We have used the thermal predictions of this model for comparison with the sample values for these wells. The assumption is made that thermal conditions within the basin are laterally uniform to the degree that projection from the sample well to the appropriate equivalent location on the model cross section is valid. It may, in theory, be possible to achieve greater accuracy by modelling the section at each of the wells in detail, but our concern here is the degree to which sparse information used in the model can be extrapolated to adjacent regions of the basin. Given the uncertainties if both the reaction kinetics and the model predictions, this approach is the easiest to justify.

Model thermal results

Only the thermal properties of the sediments have been varied in the models of this section to achieve agreement between observed corrected bottom-hole temperatures in the sample wells, a.–i. reaction extents and measured values of the thermal conductivity and radiogenic heat production of representative sediments from the Nova Scotian margin.

Table 3 lists the parameter values used and figure 6 illustrates the sensitivity of model predictions of current geothermal gradients at one sample well, Bluenose, to the parameter values and compares them with corrected bottom-hole temperatures for that well (Issler 1984*a* and personal communication). As noted previously, the subsidence history of the basin was largely insensitive to the range of thermal properties of the sediments used and so the values of the stretching factors, β and δ, for each of the wells are constant.

PHILOSOPHICAL TRANSACTIONS OF THE ROYAL SOCIETY A MATHEMATICAL, PHYSICAL & ENGINEERING SCIENCES

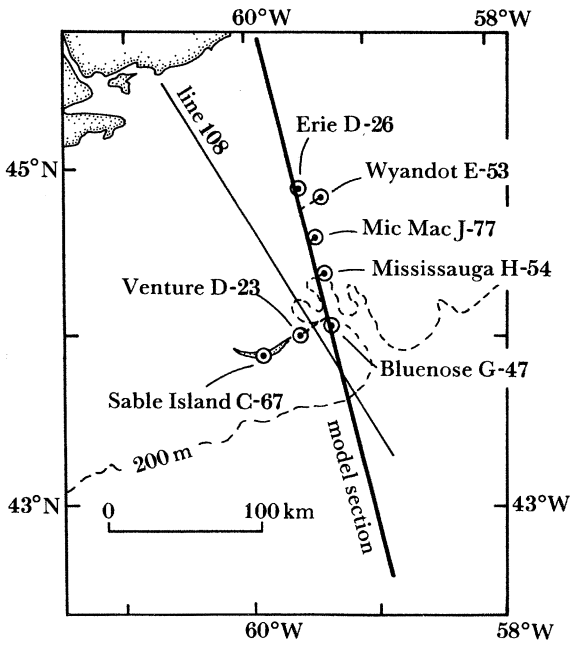

FIGURE 5. Location map of the Nova Scotian margin showing the wells from which a.–i. samples were taken in relation to the modelled cross section.

TABLE 3. PARAMETER AND PROPERTY VALUES FOR SEDIMENTARY LAYERS OF THE MODELS

	sandstone	shale	limestone	salt
matrix density, ρ_{sg}/(kg m^{-3})	2650	2700	2710	2160
compaction constant, h m^{-1}	360	650	160	∞
surface porosity, ϕ_0 (percentage)	62	60	24	0
thermal conductivity, K				
Beaumont *et al.* (1982*a*)				
(Wm^{-1} K^{-1})	4.184	1.883	2.929	5.858
(kcal[a] cm^{-1} s^{-1} K^{-1})	10	4.5	7	14
model A				
(Wm^{-1} K^{-1})	2.761	1.255	1.925	5.858
(kcal cm^{-1} s^{-1} K^{-1})	6.6	3.0	4.6	14
model B				
(Wm^{-1} K^{-1})	2.552	1.130	1.757	5.858
(kcal cm^{-1} s^{-1} K^{-1})	6.1	2.7	4.2	14
specific heat, c				
(J kg^{-1} K^{-1})	1088	837	1004	854
(cal gm^{-1} K^{-1})	0.26	0.20	0.24	0.204
radiogenic heat production, A				
(μW m^{-3})	0.8368	1.046	0.8368	0
10^{10}(kcal cm^{-3} s^{-1})	2	2.5	2.0	0

[a] 1 cal = 4.1868 J.

A simple approach is used for calculating the net thermal conductivity of the sediment column at each location. Each lithology is assigned mineral matrix thermal properties (table 3). The geometric mean of these values is then used for the sediment added at each time step according to the percentage of each lithology present in the sediment for that time step. Changes in

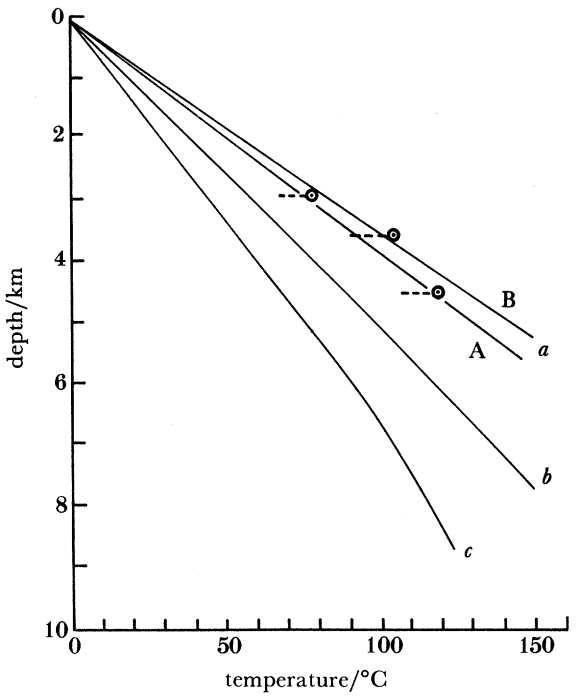

FIGURE 6. Comparison of predicted (models A and B) and observed present temperature against depth for the Bluenose G-47 well, illustrating the influence of sediment thermal conductivity and radiogenic heat production. (*a*) Modified thermal conductivity and radiogenic heat; (*b*) commonly quoted thermal conductivity and radiogenic heat; (*c*) commonly quoted thermal conductivity, no radiogenic heat.

conductivity with porosity are then computed by using the Maxwell model (Beck 1976). The mean of the thermal conductivities thus predicted, weighted by the relative thicknesses, is then used as the sediment conductivity for that column of sediment for each time step. The model therefore uses a representative 'bulk conductivity' for the sediment column.

The commonly quoted conductivity values used by Beaumont *et al.* (1982*a*), which are averages for the rock types concerned, are clearly inappropriate. They predict geothermal gradients of *ca.* 16 °C km^{-1}, consistently lower than those observed in all the wells. Addition of radiogenic heating in a near-surface (7.5 km deep) uniformly radioactive crustal layer and within the sediment column raises the geothermal gradient significantly, but the predicted values, *ca.* 20 °C km^{-1}, are still too low. The radioactive heat production of the model sediments is the mean of that observed for each lithology in samples from the Nova Scotian margin (Keen & Lewis 1982). Models having these thermal properties predicted insignificant amounts of the aromatization and isomerization reactions, even for samples taken from deep in the wells and in which the reactions are known to have gone to completion.

Much better results are given by using the sediment properties of models A and B (table 3, figure 6), which are based on laboratory measurements of representative sample thermal conductivities (C. E. Keen, personal communication).

Elimination of samples contaminated with migrated oil

Figure 8 is a plot of the extent of steroid aromatization as a function of sterane isomerization at C-20, which, following the convention of Mackenzie & McKenzie (1983), will be referred

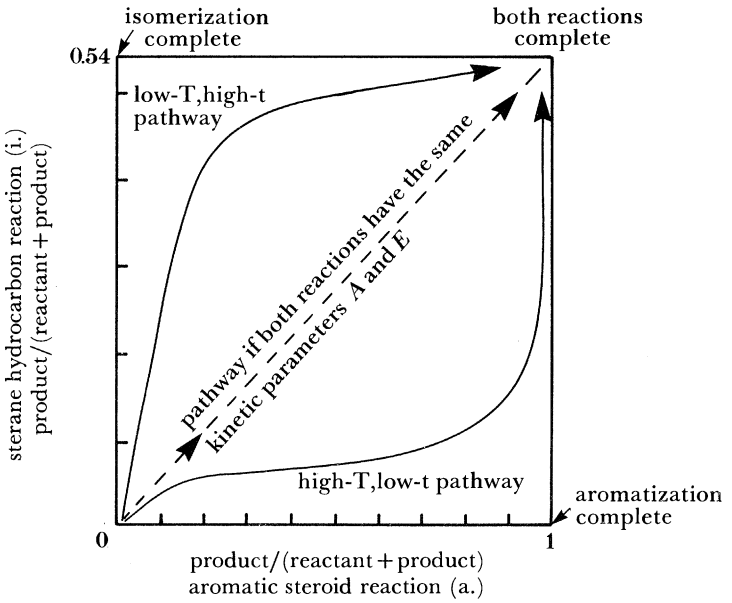

FIGURE 7. The a.–i. diagram. Reactions start in the lower left corner of the diagram and proceed to completion in the upper right corner. The axes are labelled by progress of the reaction toward completion or equilibrium. Reaction pathways in the diagram are diagnostic of the temperature histories of the samples. Histories involving large elapsed time in a relatively cool (less than *ca.* 95 °C) environment favour progress of the isomerization reactions toward completion before that of the steroid aromatization and, therefore, paths are in the upper left of the figure. Conversely, histories involving short elapsed time in a relatively hot environment (greater than *ca.* 100 °C) favour the rapid completion of the steroid aromatization and, therefore, paths are in the lower right of the diagram.

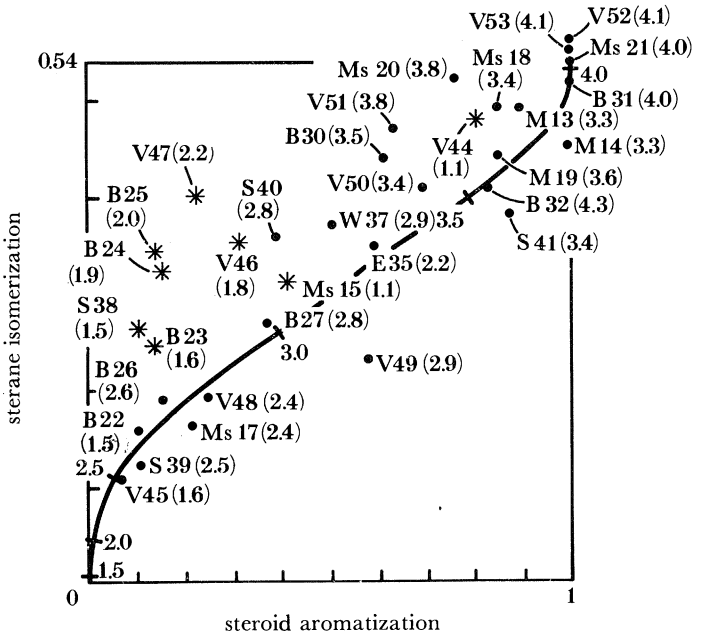

FIGURE 8. An a.–i. diagram showing the observed amounts of reaction for the samples from the Nova Scotian margin compared with the average trend of reaction against depth beneath the shelf region. The sample depths in kilometres are shown in brackets and the average depth progression of the reactions are shown by cross bars labelled by the depth in kilometres. ●, Indigenous; *, contains migrated oil.

to as an a.–i. diagram. It is explained by figure 7. When plotted in this manner, the effects of temperature and time can be partly separated because of differences in the kinetic parameters of the steroid aromatization and sterane isomerization reactions. The a.–i. diagram can also be used to detect whether a sample contains migrated oil. Table 1 shows that, with two exceptions, all samples contain low amounts of organic carbon (less than 2%); they are susceptible to impregnation with migrated oil. There are two effects caused by the migrated oil on the position of sample results in the a.–i. diagram.

In most cases, migrated oil comes from greater depths and it is more mature than the organic matter indigenous to the sediment that it impregnates. Hence, its position in the a.–i. diagram will be correspondingly more mature than that predicted by the thermal history models and reaction constants previously discussed.

The second effect is related to the effect of mixing of a migrated crude oil with the indigenous organic matter on the actual sample position in the a.–i. diagram. Mackenzie *et al.* (1985) reported detailed quantitative studies of steroid hydrocarbons in typical extracts of sedimentary rocks and crude oils. Although no samples from the Nova Scotian margin were included in the survey, they observed that steranes are up to ten times more abundant than aromatic steroid hydrocarbons in most crude petroleums, while the converse is true for rock extracts not impregnated with crude oil. This difference is because steranes survive the maturation and migration of oil better than their aromatic steroid equivalents; the latter are preferentially degraded at elevated temperature and retained by the rocks through which the oil passes. Hence, progressive mixing of a mature crude oil with an immature rock extract will initially increase the isomerization value (measured on steranes in the extract) and then increase the aromatization value (measured on aromatic steroid hydrocarbons). The mixing curve of an immature extract, in the bottom left of the a.–i. diagram, with a mature oil, in the top right of the diagram, will fall above the maturation trend that connects them.

The a.–i. results for the Nova Scotia samples are shown in figure 8 together with their depths and the general trend of the reactions predicted by model B. The reactions are predicted to occur principally between 2.5 and 3.5 km. Sample results, plotted as asterisks, are considered to contain migrated oil, for the reasons outlined above and these samples are noted in table 1. Those shown as solid dots are considered to be unaffected by impregnation with migrated oil; their position on the a.–i. diagram is purely a consequence of the chemical reactions which have occurred in the rock itself. The impregnated samples mainly come from a depth range of 1.3–2.3 km, depths for which oil staining is often detected in cores from the Nova Scotian margin and the interval in which some of the small oil finds of the area occur. Most of these sample results were rejected because the reactions were too advanced for their depths (such as Venture V44). Samples from the Sable S38 well, the Bluenose well from B23 to B25 and the Venture well V46 and V47 show clear mixing trends; their isomerization values have been systematically increased away from the main maturation trend.

Well age–depth and temperature–depth results

Having decided on the samples whose a.–i. values represent the reaction of indigenous components and not the effect of migrated oil and that models A and B give general agreement with the temperature date, it is now possible to examine individual wells and well grouping in more detail. The results are arranged as four panels in each of figures 9–14.

Parts *a*, figures 9–14, compare the theoretical (dots) and observed (crosses) present

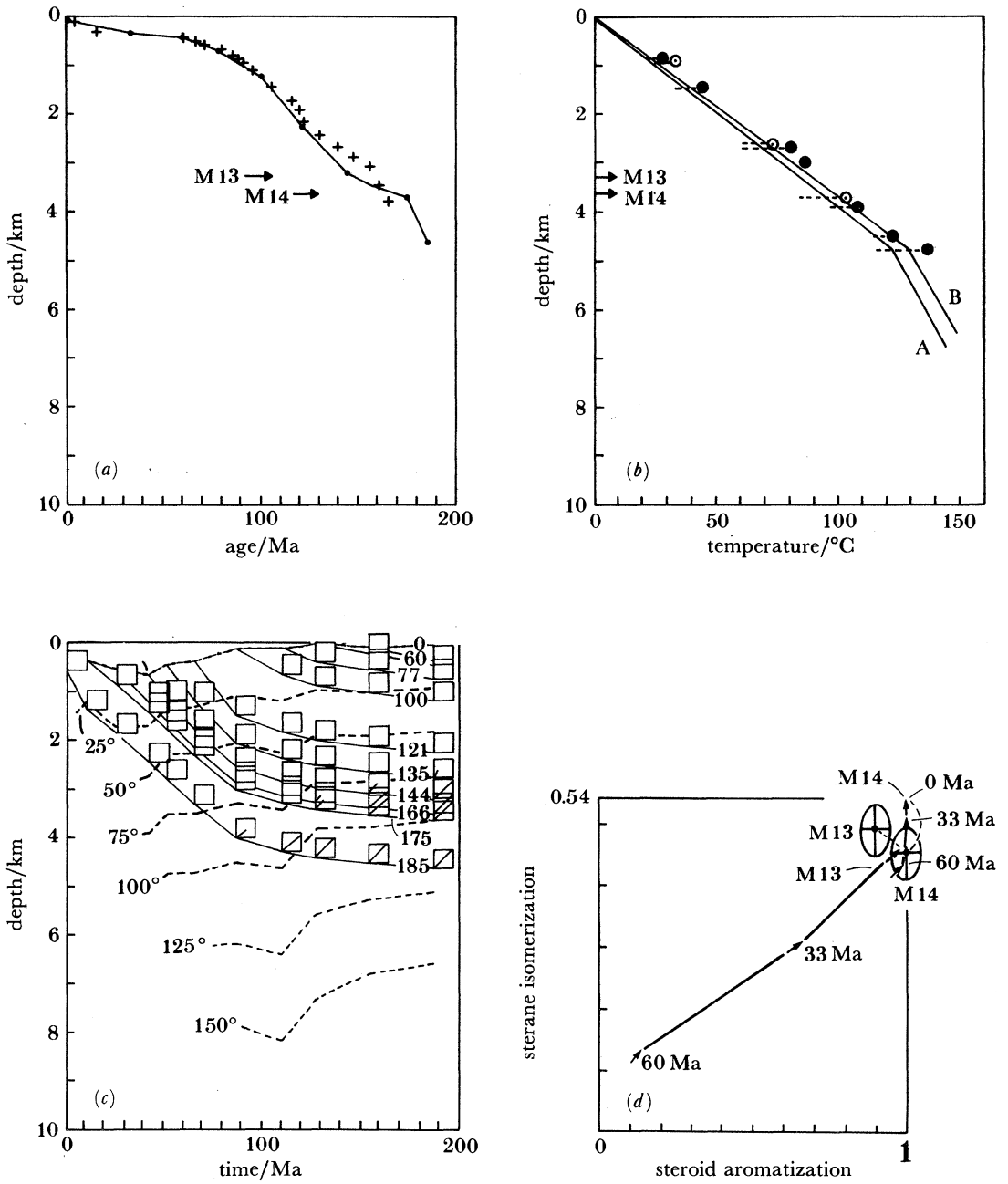

FIGURE 9. Diagram showing comparison of model predictions with observations from the Mic-Mac H-86 and J-77 wells, for age–depth and temperature–depth relations. (*a*) +, Mic Mac J-77; (*b*) ●, Mic Mac H-86; ⊙, Mic Mac J-77. See text for details. Broken lines show temperatures in degrees Celsius.

age–depth relations. Uncertainties in the biostratigraphic ages and depths of the samples are, on average, approximately equal to the size of the crosses. Uncertainties in the conversion from stratigraphic age to absolute age are a little larger and the results are in better agreement with observations if the Harland *et al.* (1982) time scale is used instead of the D.N.A.G. (Decade of North American Geology) scale (Palmer 1983). The results presented here are, however, acceptable. The depths from which the a.–i. samples were taken are also shown.

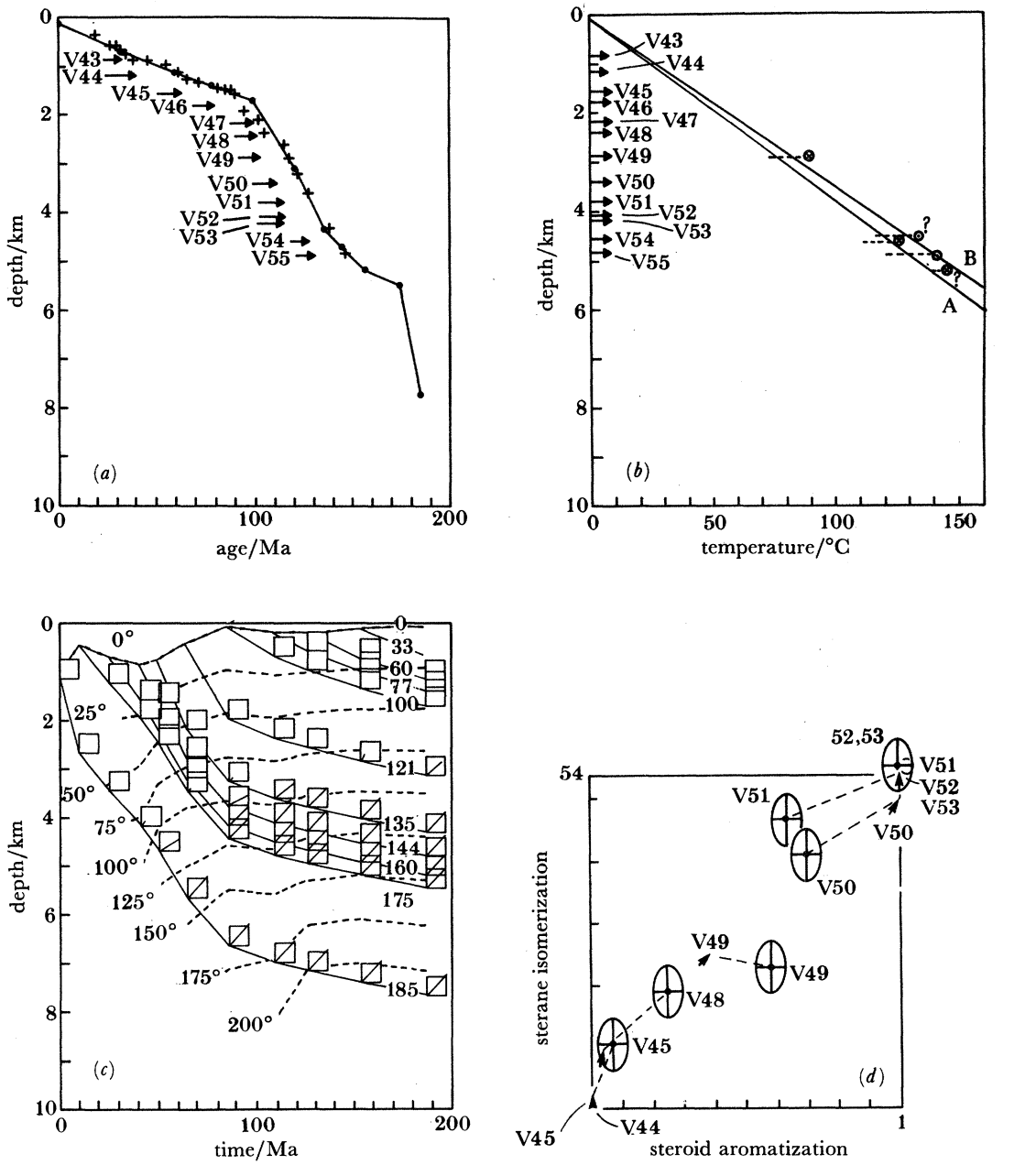

FIGURE 10. The same composite diagram as figure 9, but for the Venture D-23 well. In (*b*), ⊙ represents Venture D-23 (all samples); ⊗ represents Venture B-13.

In part *b* of each figure, the predicted present temperature distribution of models A and B is compared with observed corrected bottom-hole temperatures. The size of the corrections, which revise the observed temperatures upward to correct for the cooling effect of drilling mud circulation (Issler 1984*a*) are shown by the broken lines. The least reliable corrections are labelled with a question mark. Both models are in reasonably good agreement with the observations, which do not indicate other than a uniform gradient within the sediments. The predicted near-surface temperatures may be up to 5 °C low and both models may predict a slightly low temperature for the Mic Mac H-86 well.

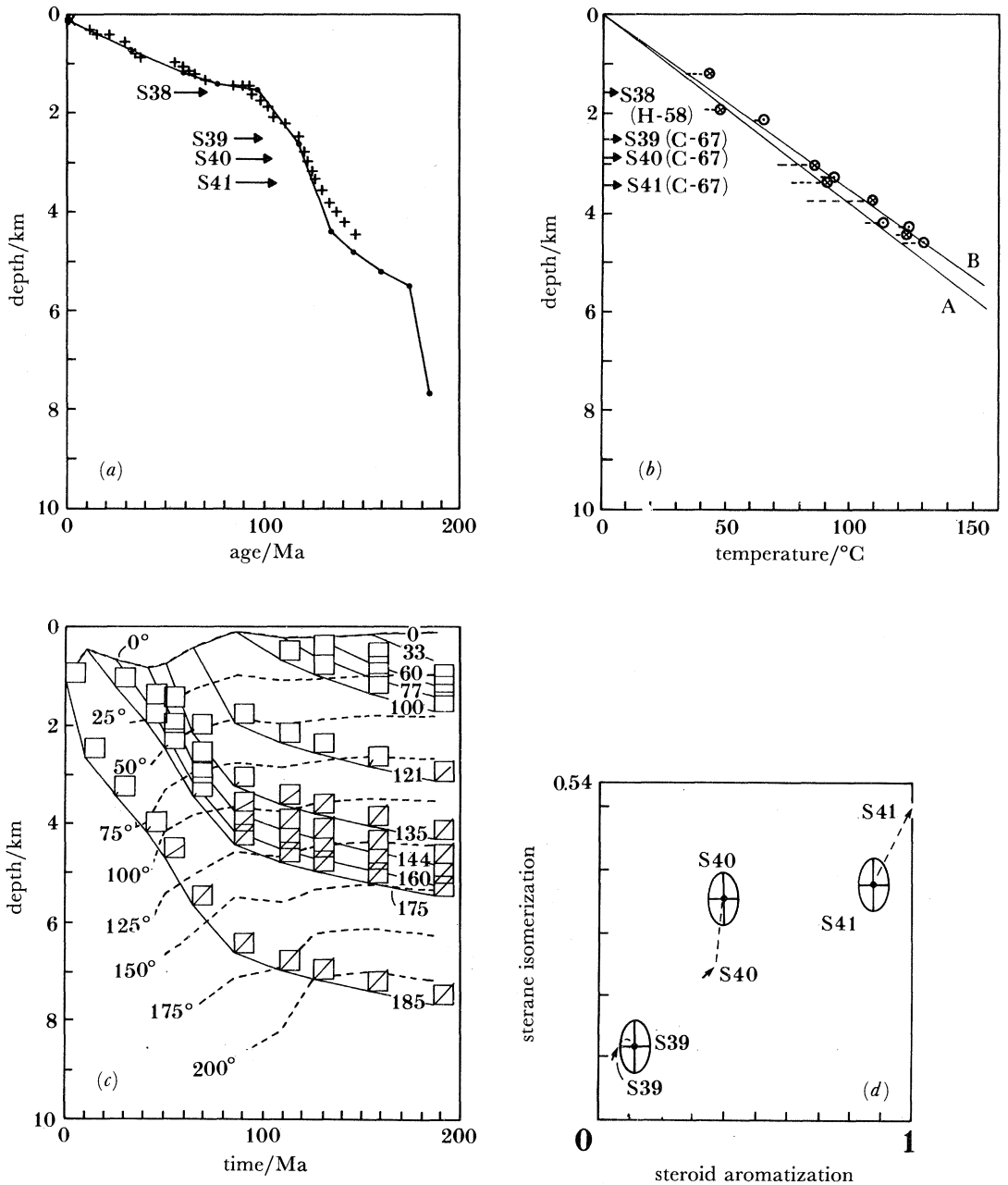

FIGURE 11. The same composite diagram as figure 9, but for the Sable Island C-67 and H-58 wells. In (*b*), ⊙, represents Sable C-67; ⊗ represents Sable H-58.

Parts *c* show the subsidence, temperature and a.–i. reaction histories for each well. The solid lines trace the subsidence history of the model B stratigraphic horizons as a function of time since rifting. Their present depths are labelled with the age, in millions of years. The corresponding changes in temperature distribution with time (broken lines) partly reflect changing paleobathymetry shown by the depth of the 0 °C isotherm and are also related to basal heat flux, sediment lithology and compaction, and radiogenic heat production.

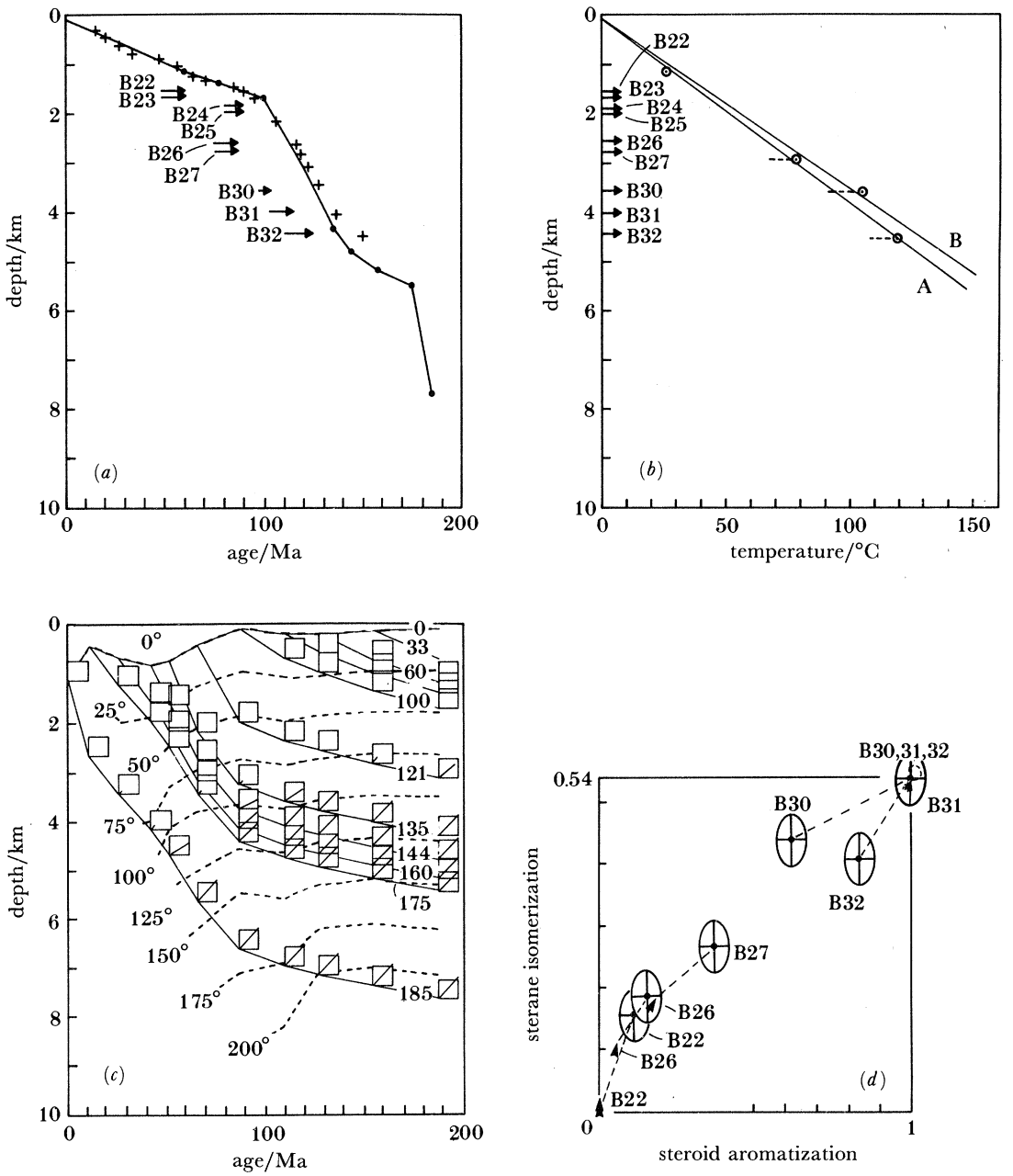

FIGURE 12. The same composite diagram as figure 9, but for the Bluenose G-47 well.

Model a.–i. *results*

In the small boxes of the parts *c* are a.–i. diagrams showing the progress of the sterane isomerization and steroid aromatization reactions. As explained in figure 8, reaction paths progress from the bottom left to top right corners and the straight lines in each of the boxes of parts *c* join the predicted reaction endpoints to the origin; they do not show the reaction path in the diagram. The boxes refer to the time–depth–temperature location of their bottom left corners. For example, in the Mic Mac well, reactions in sediment 185 Ma old are predicted to have started 80 Ma after rifting and to be complete by 130 Ma. Reactions are currently

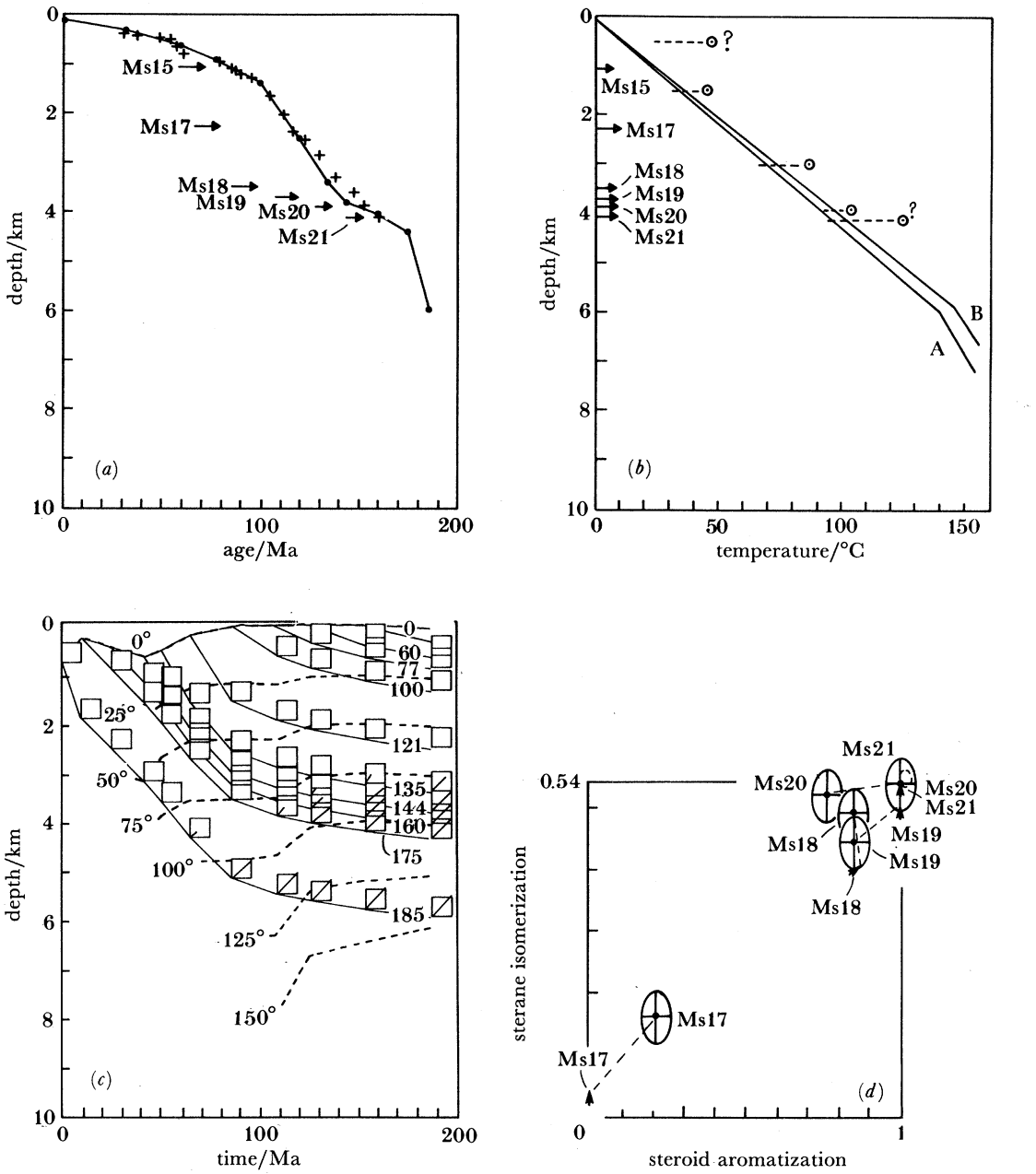

FIGURE 13. The same composite diagram as figure 9, but for the Mississauga H-54 well.

underway in sediments that are 135 ± 10 Ma old at depths of *ca.* 2.8 ± 0.5 km. The reactions, once started, are very sensitive to temperature and time and, for the Nova Scotian margin, typically traverse the a.–i. diagram in a depth range of 1 km. This sensitivity means that even to have captured the reactions in progress within a sample, irrespective of their precise relative amounts, provides a good measure of the approach to the onset of maturity.

Parts *d* compare the observed sample (⊕) and corresponding predicted (↑) states of the reactions when taken in pairs and plotted as a.–i. diagrams. The discrepancy between predictions, mostly those for model B, and observation is shown by a broken line.

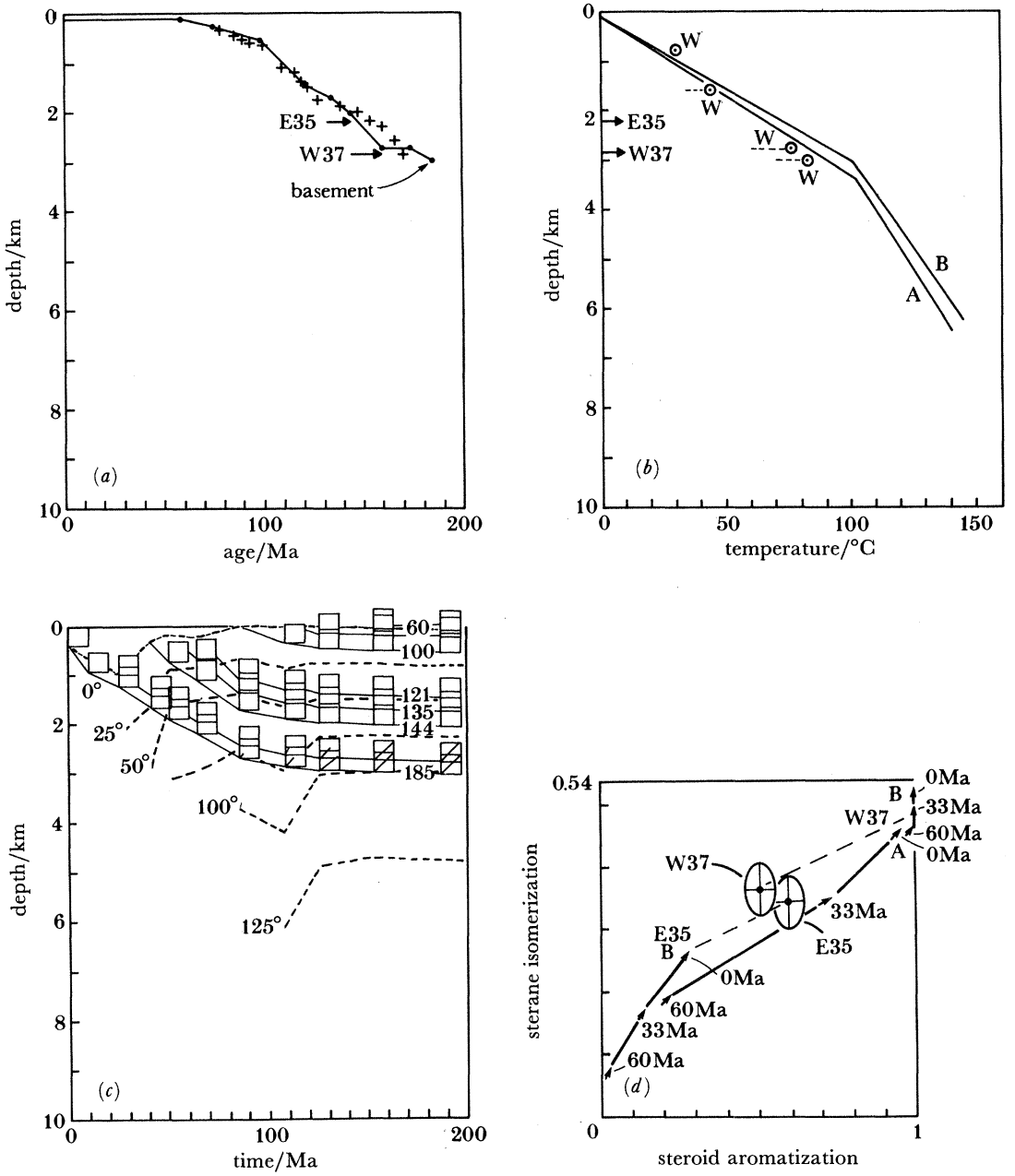

FIGURE 14. The same composite diagram as figure 9, but for the Erie D-26 and Wyandot E-53 wells. In (*a*), + represents Wyandot and ● represents Erie.

In Mic Mac samples M13 and 14, reactions are nearly complete, as predicted, and there is sufficient space to show the predicted progress of the reactions from 60 to 33 Ma ago and then to present by a series of three arrows joined by a bold solid line. Note the large difference in amount of reaction during this period for the two samples; reactions for M14, the deeper sample, were approaching completion even 60 Ma ago. During the last 60 Ma, the thermal gradient has remained almost constant (figure 9*c*) but the sample temperatures have increased by *ca.* 10 °C as a result of blanketing by the 400 m of sediment deposited. Both temperature and time

are contributing to the reactions; late stage subsidence evidently plays an important role in determining the depth to mature sediments. Observed and predicted results for the reactions for both samples are in good agreement; the reactions being insensitive to small errors in their early temperature history which result from differences between the observed and predicted subsidence history (figure 9*a*).

The Venture D-23 well was studied in greater detail because it is important in relation to the Venture gas field. The ten samples not impregnated with migrated oil show the effects of *in situ* reactions in the sediments. The model accurately predicts the present age–depth curve and temperature–depth observations (figure 10). Part *c* indicates that virtually no a.–i. reactions should have occurred in sample V45, which comes from a depth where the temperature is low. Correspondingly, reactions in samples V51-V55, which come from depths of 4 km or more, should be nearing completion; samples V48-V50 are intermediate. Part *d* confirms these predictions.

The results for the Sable Island (C-67) samples S39-S41 (figure 11) again show good correspondence between theoretical and observed stratigraphy and present temperature, particularly for model B. The samples all come from depths for which reactions are predicted to be in progress (*c*) and the observations confirm this prediction (*d*). Sample S38, from the Sable Island (H-58), however, shows a greater degree of reaction than predicted, particularly for the isomerization (figure 8). The pattern of enrichment suggests impregnation of this sample by migrating oils and it was not included in the results of figure 11.

Similar encouraging agreements occur for the Bluenose, Mississauga and Wyandot wells (figures 12–14).

Temperature and maturation of the Nova Scotian margin sediments

The results from all the wells that were part of the a.–i. study are best summarized by projecting the temperature and reaction distributions on the model cross section (figures 3 and 15). The temperature distribution (top panel, figure 3) is for model B, which agrees best with observations where available. At depths greater than 4 km, and in all areas below the

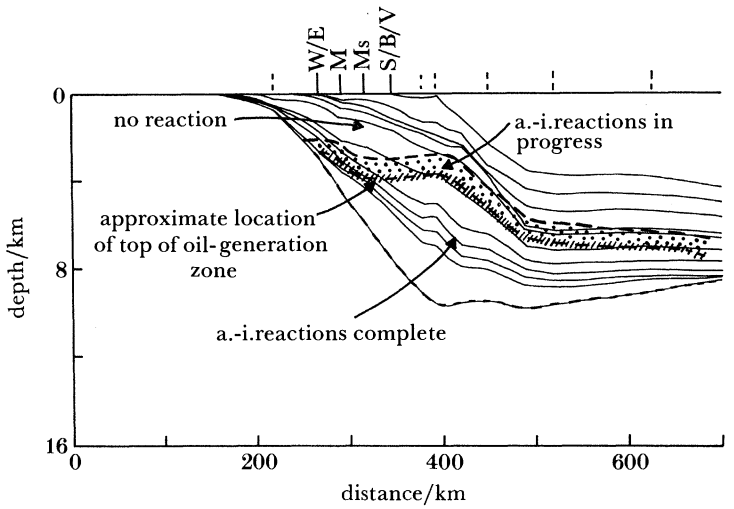

Figure 15. Model B prediction of the region in which the a.–i. reactions are presently underway. The well locations are shown at the top of the diagram.

continental slope and rise, the results are theoretical predictions based on the good agreement elsewhere and the assumption that shale is the dominant lithology beneath the slope and rise. Figure 15 shows that the a.–i. reactions are currently underway in a thin (*ca.* 1 km) zone that crosses stratigraphic horizons. Its depth is correct where drilling results are available. Beneath the slope and rise the zone position has been predicted by using the theoretical temperature history and the reaction kinetics.

Much more work is necessary to relate the basin temperature history to oil and gas maturation, but present results serve to calibrate and give confidence to the theoretical temperature predictions. Such results will also help in quantifying the relation between other geochemical indicators, including oil and gas formation from kerogen with temperature and time.

The a.–i. reactions used in this study occur before significant oil and gas generation. On the basis of the knowledge (Mackenzie & Maxwell 1981) that the onset of significant petroleum generation corresponds to the completion of the reactions, it is possible to map an approximate distribution of the top of the zone of petroleum generation and to predict the timing of generation (figure 3) for the cross section of the Nova Scotian margin. This distribution is approximate because it considers only the largest scale structure of the basin. It does not include small-scale perturbations that may occur as a result of local variations in lithology, sediment thickness or salt–shale diapirism.

In a detailed geochemical study of oils and condensates produced from the Scotian Shelf, Powell (1982) proposed that most of the oils and condensates were expelled from the Verrill Canyon formation when it reached the maturity equivalent to 0.7 and 0.9% vitrinite reflectance. The average depth for 0.7% reflectance in these wells is 4 km, which agrees well with the location of the top of the oil-generation zone predicted by the model for the shelf region (figure 3, top panel).

The good agreement between present levels of observed and predicted maturation encourages us to use the model to predict the timing of oil generation in the Verrill Canyon formation along the model cross section. Figure 3 shows the temperature history (broken lines) and movement of the upper boundary of the oil-generation zone (solid underscored line), taken to be the depth at which the a.–i. reactions go to completion. The Verrill Canyon formation (shaded area) entered the oil-generation zone as early as the Barremian in the area beneath the slope and outer shelf, and there was a steady increase in the thickness of potential source rocks during the Early Cretaceous, reflecting uniform rates of sedimentation (parts *a*, figures 9–14).

The Late Cretaceous was a time when sedimentation rates decreased by a factor of approximately two; correspondingly, the amount of sediment predicted to have been added to the oil-generation zone during this time is less than that during the Early Cretaceous.

The amount of sediment entering the oil-generation zone during the Tertiary increases significantly with proximity to the edge of the shelf. Heat flux had stabilized by this time and the reactions respond to increasing temperature that stems from increased thermal blanketing by additional sediments. Locations shoreward of the Mic Mac well received little sediment, therefore, the a.–i. reactions progressed slowly (figure 14*d*) and only *ca.* 300 m of sediment entered the oil-generation zone. For the Mic Mac well, the corresponding figure is *ca.* 400 m. The slow progress of the a.–i. reactions for samples M13 and 14 (figure 9*d*) illustrates this result and that the top of oil-generation zone begins at *ca.* 3.8 km, the depth of sample M14.

Between 1.2 and 1.5 km of sediment entered the oil-generation zone during the Tertiary

PHILOSOPHICAL TRANSACTIONS OF THE ROYAL SOCIETY A MATHEMATICAL, PHYSICAL & ENGINEERING SCIENCES

beneath the Bluenose, Venture and Sable Island wells. Calculations indicate that the a.–i. reactions for samples such as B31-32 and V52-55 progressed rapidly to completion during this period and that the present depth to the top of the oil-generation zone in this area is also 3.8–4.0 km. Significantly, less sediment is predicted to have entered the oil-generation zone beneath the continental slope and rise than beneath the outer shelf during the Tertiary. The top of this zone approximately parallels chronostratigraphic horizons in this region, as do the isotherms; whereas beneath the shelf both these sets of contours cut across the model stratigraphy.

These predictions are in agreement with Powell's (1982) conclusions. The Verrill Canyon shales are mature within the Sable Subbasin. Their potential as source rocks depends of course on their organic carbon content. Overlying formations, such as the Logan Canyon and Wyandot, in which small pools of oil and condensates have been discovered (see Powell (1982) for a review of these accumulations and primary references), are not predicted to be mature. The Late Cretaceous Wyandot formation is not predicted to have entered the zone of a.–i. reaction and the Logan Canyon formation is in the a.–i. reaction zone only at the base of the slope.

Conclusions

We have compared the measured extents of geochemical reactions in 33 sediment samples from offshore Nova Scotia with the extents predicted by a numerical model of the burial and thermal histories of the sediments. Agreement between the observations and predictions is, in general, good if the values used for the thermal properties of the sediments are based on laboratory measurement of representative samples of the sediments concerned and not on commonly quoted standard values from the literature. Under these circumstances, good agreement was also obtained between predicted and observed bottom-hole temperatures. Some sediments recorded anomalously high reaction extents for their depth; we ascribe this to impregnation by oil which has migrated from depth.

The good agreement between observations and predictions suggests the modelling used is, to a first approximation, correct; the activation energies and frequency factors of the geochemical reactions derived previously by Mackenzie & McKenzie (1983) also explain the observations from the Nova Scotia margin.

The model and geochemical reaction constants may be used to predict subsidence and temperature histories, and reaction extents for regions where there is no sample control. Such an exercise demonstrates the importance of both temperature and time in causing the reactions.

The thermal model was also used tentatively to reconstruct oil generation from what is considered to be the principal source rock of the region, the Middle Jurassic to Lower Cretaceous Verrill Canyon formation. The current top of the oil-generation zone is at a depth of 3.8–4 km beneath the outer shelf and uppermost slope regions. Oil generation in the Verrill Canyon shales is predicted to have commenced in the Barremian and to have continued to the present. The overlying Logan Canyon and Wyandot formations are not predicted to be regions of significant oil generation. Apart from the possibility of local spots of maturation, where thermal conditions may have been anomalous by comparison with basin averages, oils and condensates in these formations have migrated to their present positions.

PHILOSOPHICAL TRANSACTIONS OF THE ROYAL SOCIETY A MATHEMATICAL, PHYSICAL & ENGINEERING SCIENCES

We thank Graham Williams, Art Jackson and Kim Duffy of the Bedford Institute of Oceanography, Dartmouth, N.S. and Trevor Powell, formerly of the Institute of Sedimentary and Petroleum Geology, Calgary, Alberta, for help in obtaining the samples used in this study and for advice and useful discussions. A.S.M. and J.R. gratefully acknowledge the technical assistance of U. Disko, B. Kammer, F. Schlosser, J. Schnitzler and the support of Professor D. H. Welte. Some additional and confirmatory analyses were done at the BP Research Centre. We thank G. P. Cooles and N. S. Goodwin for assistance with the analyses, and BP p.l.c. for permission to publish the results. A.S.M. thanks the Alexander-von-Humbolt Foundation for a fellowship. C.B. thanks Professor Ron Oxburgh and the Department of Earth Sciences, Cambridge University, for hospitality during his stay and St John's College for a Commonwealth Fellowship. Financial support was provided through a Strategic Grant and Steacie Fellowship from the Natural Sciences and Engineering Research Council, Canada, to C.B.

References

Bally, A. W. 1982 Musings over sedimentary basin evolution. *Phil. Trans. R. Soc. Lond.* A **305**, 325–338.

Bally, A. W., Bernoulli, D., Davis, G. A. & Montadert, L. 1981 Listric normal faults. *Oceanologica Acta* 87-102.

Beaumont, C., Boutilier, R., Mackenzie, A. S. & Rullkötter, J. 1985 Isomerization and aromatization of hydrocarbons and the paleothermometry and burial history of the Alberta foreland basin. *Am. Assoc. Pet. Geol. Bull.* (In the press.)

Beaumont, C., Boutilier, R. & Keen, C. E. 1984 Marginal models. In *Petroleum Geology of the North European Margin* (ed. A. M. Spencer), pp. 171–187.

Beaumont, C., Keen, C. E. & Boutilier, R. 1982*a* On the evolution of rifted continental margins: comparison of models and observations for the Nova Scotian margin. *Geophys. Jl R. astr. Soc.* **70**, 667–715.

Beaumont, C., Keen, C. E. & Boutilier, R. 1982*b* A comparison of foreland and rift margin sedimentary basins. *Phil. Trans. R. Soc. Lond.* A **305**, 295–317.

Beck, A. E. 1976 An improved method of computing the thermal conductivity of fluid-filled sedimentary rocks. *Geophysics* **41**, 133–144.

Bodine, J. H. 1981 The thermo-mechanical properties of oceanic lithosphere. Ph.D. thesis, Columbia University, New York, USA.

Bodine, J. H., Steckler, M. S. & Watts, A. B. 1981 Observations of flexure and the rheology of the oceanic lithosphere. *J. geophys. Res.* **86**, 3695–3707.

de Bremaecker, J.-Cl. 1983 Temperature, subsidence, and hydrocarbon maturation in extensional basins: a finite element model. *Am. Assoc. Pet. Geol. Bull.* **67**, 1410–1414.

Courtney, R. C. & Beaumont, C. 1983 Thermally activated creep and flexure of the oceanic lithosphere. *Nature, Lond.* **305**, 201–204.

Dastillung, M. & Albrecht, P. 1977 Δ^2-steranes as diagenetic intermediates in sediments. *Nature, Lond.* **269**, 678–679.

Ensminger, A., Albrecht, P., Ourisson, G. & Tissot, B. 1977 Evolution of polycyclic alkanes under the effects of burial (early Toarcian shales, Paris Basin). In *Advances in organic geochemistry* 1975 (ed. R. Campos & J. Goni), pp. 45–52. Madrid: ENADIMSA.

Ensminger, A., Van Dorsselaer, A., Spyckerelle, C., Albrecht, P. & Ourisson, G. 1974 Pentacyclic triterpanes of the hopane type as ubiquitous geochemical markers: origin and significance. In *Advances in organic geochemistry* 1973 (ed. B. Tissot & F. Bienner), pp. 245–260. Paris: Editions Technip.

Foucher, J.-P. le, Pichon, X. & Sibuet, J.-C. 1982 The ocean-continent transition in the uniform lithospheric stretching model: role of partial melting in the mantle. *Phil. Trans. R. Soc. Lond.* A **305**, 27–40.

Garven, G. & Freeze, R. A. 1984*a* Theoretical analysis of the role of groundwater flow in the genesis of stratabound ore deposits. Part 1: mathematical and numerical models. *Am. J. Sci.* (In the press.)

Garven, G. & Freeze, R. A. 1984*b* Theoretical analysis of the role of groundwater flow in the genesis of stratabound ore deposits. Part 2: quantitative results. *Am. J. Sci.* (In the press.)

Gunstone, F. D. 1974 *Basic stereochemistry*. London: English Universities Press.

Harland, W. B., Cox, A., Llewellyn, P. G., Pickton, C. A. G., Smith, A. G. & Walters, R. 1982 *A geological time scale*. Cambridge University Press.

Hitchon, B. 1984 Geothermal gradients, hydrodynamics, and hydrocarbon occurrences, Alberta, Canada. *Am. Assoc. Pet. Geol. Bull.* **68**, 713–743.

Hood, A., Gutjahr, C. C. M. & Heacock, R. L. 1975 Organic metamorphism and the generation of petroleum. *Am. Assoc. Pet. Geol. Bull.* **59**, 986–996.

PHILOSOPHICAL TRANSACTIONS OF THE ROYAL SOCIETY A MATHEMATICAL, PHYSICAL & ENGINEERING SCIENCES

Issler, D. R. 1984*a* Calculation of organic maturation levels for offshore eastern Canada – implications for general application of Lopatin's method. *Can. J. Earth Sci.* **21**, 477–488.

Issler, D. R. 1984*b* An investigation of the thermal and subsidence history of the Labrador Margin. *Joint programme with abstracts, 18th Annual CMOS Congress–11th Annual CGU Meeting, Halifax, Nova Scotia, Canada.* P. 98.

Jarvis, G. T. & McKenzie, D. P. 1980 Sedimentary basin formation with finite extension rates. *Earth planet. Sci. Lett.* **48**, 42–52.

Keen, C. E. 1979 Thermal history and subsidence of rifted continental margins – evidence from wells on the Nova Scotian and Labrador shelves. *Can. J. Earth Sci.* **16**, 505–522.

Keen, C. E. & Lewis, T. 1982 Radiogenic heat production from the continental margin of eastern North America: Implications for petroleum generation. *Am. Assoc. Pet. Geol. Bull.* **66**, 1402–1407.

Mackenzie, A. S., Rullkötter, J. & Welte, D. H. 1985 Correlation of oils and source rocks, North Slope Alaska. In *North Slope oil-rock correlation study, A.A.P.G. Spec. Pub.* (ed. L. Magoon & G. Claypool). (In the press.)

Mackenzie, A. S. & McKenzie, D. P. 1983 Isomerization and aromatization of hydrocarbons in sedimentary basins formed by extension. *Geol. Mag.* **120**, 417–528.

Mackenzie, A. S., Disko, U. & Rullkötter, J. 1983 Determination of hydrocarbon distributions in oils and sediment extracts by gas chromatography–high resolution mass spectrometry. *Org. Geochem.* **5**, 57–63.

Mackenzie, A. S., Brassell, S. C., Eglinton, G. & Maxwell, J. R. 1982 Chemical fossils – the geological fate of steroids. *Science, Wash.* **217**, 491–505.

Mackenzie, A. S. & Maxwell, J. R. 1981 Assessment of thermal maturation in sedimentary rocks by molecular measurements. In *Organic maturation studies and fossil fuel exploration* (ed. J. Brooks), pp. 239–254. London: Academic Press.

McKenzie, D. P. 1981 The variation of temperature with time and hydrocarbon maturation in sedimentary basins formed by extension. *Earth planet. Sci. Lett.* **55**, 87–98.

McKenzie, D. P. 1978 Some remarks on the development of sedimentary basins. *Earth planet. Sci. Lett.* **40**, 25–32.

Montadert, L., de Charpal, O., Roberts, D., Guennoc, P. & Sibuet, J.-C. 1979 Northeast Atlantic passive continental margins: rifting and subsidence processes. In *Maurice Ewing Symposium Series*, vol. 3, pp. 154–186. American Geophysics Union.

Ourisson, G., Albrecht, R. & Rohmer, M. 1979 The hopanoids: paleochemistry and biochemistry of a group of natural products. *Pure appl. Chem.* **51**, 709–729.

Oxburgh, E. R. & Andrews-Speed, C. P. 1981 Temperature, thermal gradients, and heat flow in the south western North Sea. In *Petroleum geology of the continental shelf of North West Europe* (ed. L. V. Illing & G. D. Hobson), pp. 141–151. London Institute of Petroleum.

Palmer, A. R. 1983 The Decade of North American Geology 1983 geologic time scale. *Geology* **11**, 503–504.

Parsons, B. & Sclater, J. G. 1977 An analysis of the variation of ocean floor bathymetry and heat flow with age. *J. geophys. Res.* **82**, 803–827.

Powell, T. G. 1982 Petroleum geochemistry of the Verrill Canyon formation: a source for Scotian Shelf hydrocarbons. *Bull. Can. Petrol. Geol.* **30**, 167–179.

Rhead, M. M., Eglinton, G. & Draffen, G. H. 1971 Hydrocarbons produced by the thermal alteration of cholesterol under conditions simulating the maturation of sediments. *Chem. Geol.* **8**, 277–297.

Royden, L. & Keen, C. E. 1980 Rifting processes and thermal evolution of the continental margin of eastern Canada determined from subsidence curves. *Earth planet. Sci. Lett.* **51**, 343–361.

Royden, L., Sclater, J. G. & Von Herzen, R. P. 1980 Continental margin subsidence and heat flow, important parameters in formation of petroleum hydrocarbons. *Am. Assoc. Pet. Geol. Bull.* **64**, 173–187.

Sawyer, D. S., Swift, B. A., Sclater, J. G. & Toksöz, M. N. 1982 Extensional model for the subsidence of the northern United States Atlantic continental margin. *Geology* **10**, 134–140.

Sawyer, D. S., Toksöz, M. N., Sclater, J. G. & Swift, B. A. 1983 Thermal evolution of the Baltimore Canyon Trough and Georges Bank Basin. *Am. Assoc. Pet. Geol. Mem.* **34**, 743–764.

Sclater, J. G. & Christie, P. A. F. 1980 Continental stretching: an explanation of the post Mid-Cretaceous subsidence of the Central North Sea Basin. *J. geophys. Res.* **85**, 3711–3739.

Seifert, W. K. & Moldowan, J. M. 1980 The effect of thermal stress on source rock quality as measured by hopane stereochemistry. In *Advances in organic geochemistry* 1974 (ed. A. G. Douglas & J. R. Maxwell), pp. 229–237. Oxford: Pergamon Press.

Steckler, M. S. 1981 The thermal and mechanical evolution of Atlantic-type continental margins. Ph.D. thesis, Columbia University, New York, USA.

Turcotte, D. L. & Angevine, C. L. 1982 Thermal mechanisms of basin formation. *Phil. Trans. R. Soc. Lond.* A **305**, 283–294.

Turcotte, D. L. & McAdoo, D. C. 1979 Thermal subsidence and petroleum generation in the southwestern block of the Los Angeles Basin, California. *J. geophys. Res.* **84**, 3460–3464.

Van Graas, Baas, G., van der Graaf, B. & De Leeun, J. W. 1982 Theoretical organic geochemistry. 1. The thermodynamic stability of several cholestane isomers calculated from molecular dynamics. *Geochim. cosmochim. Acta* **46**, 2399–2402.

Watts, A. B., Karner, G. D. & Steckler, M. S. 1982 Lithospheric flexure and the evolution of sedimentary basins. *Phil. Trans. R. Soc. Lond.* A **305**, 249–281.

PHILOSOPHICAL TRANSACTIONS OF THE ROYAL SOCIETY A MATHEMATICAL, PHYSICAL & ENGINEERING SCIENCES

Discussion

S. A. F. Murrell (*Department of Geology, University College London*). Is the high apparent thermal conductivity Professor Beaumont found in the Alberta Basin a general feature of foreland basins? Is it connected with the salt layer in the basin?

C. Beaumont. The sediments in the region are typical clastic sediments and do not have a high conductivity. The high apparent conductivity is the result of water movement, which transports heat from the mountains into the basin. The lateral transport of fluid in such basins is common but by no means ubiquitous, because there are parts of the Alberta Basin where it may be unimportant. There is little salt in the Alberta Basin and it is not responsible for the large-scale variations in temperatures.

R. Mason (*Department of Geology, University College London*). Does the abnormal heat flow affect the temperature in the boreholes?

C. Beaumont. Yes, the effect is very obvious. The geothermal gradient is strongly perturbed in the Jurassic clastic sequence that was deposited in the foreland basin, whereas in the deeper Paleozoic sediments the temperatures are, if anything, affected in the opposite way. The water circulation penetrates to the depth of the unconformity but to a lesser degree into the carbonates below.

G. Eglinton (*Organic Geochemistry Unit, School of Chemistry, University of Bristol*). Presumably the flow of water through the clastic sediments is not very uniform, so different parts of the basin should experience different thermal histories. Does this variation explain the variability in the degree of isomerization and aromatization?

C. Beaumont. In this particular basin the water flow appears to be rather uniform in the clastic sequence and we do not see any evidence for local hot and cold regions down individual boreholes. The same seems to be true of the paleogeothermal gradient also. But in general the thermal behaviour will be controlled by the details of the water circulation, therefore there are variations with geographical position in the basin. It should be possible to study the details of the heat transport by using the geochemical reactions.

S. A. F. Murrell. Could the variation in heat flux be produced by variations in the radioactive heat-generation rate?

C. Beaumont. Such an explanation seems unlikely. The geothermal gradient changes by a factor of two across this basin and the lithologies are relatively uniform. Nor is there thought to be a large variation in the radiogenic heat production of the underlying crustal rocks.

S. A. F. Murrell. The foreland basin is formed as a consequence of crustal thickening processes and therefore initially will be cold. This situation is the opposite of that on rifted margins.

PHILOSOPHICAL TRANSACTIONS OF THE ROYAL SOCIETY A MATHEMATICAL, PHYSICAL & ENGINEERING SCIENCES

C. Beaumont. We originally decided to study foreland basins because we believed they would show how the organic reactions proceeded when the heat flow into the base of the sediments was constant. Such a problem is particularly simple to model. Initially we based our requests for samples on this model, but the predictions turned out to be completely wrong. The lithosphere beneath the basin is almost certainly in thermal equilibrium, and the heat flux into the base of the sediments is constant, as you suggest. But the heat is advected around by the water circulation. Grant Garvin, a Ph.D. student at the University of British Columbia, has recently modelled this process to show how large the perturbations can be as a function of the permeability of the sediments and the hydraulic head and finds that the predicted effects are similar to those observed.

D. P. McKenzie (*Department of Earth Sciences, University of Cambridge*). The information that Professor Beaumont obtains from modelling the organic reactions is the maximum temperature that the rocks reached and the time they spent at this temperature. He then has to use a geological model to estimate the depth at which these reactions occurred. This information cannot be obtained from the organic geochemistry. A temperature gradient of 70 °C km^{-1} seems very large. In other areas, where similar geological estimates have been made of the amount of uplift, it has been systematically underestimated. A similar problem also commonly occurs with geological estimates of horizontal displacements.

C. Beaumont. Dr McKenzie is correct, the depth of burial cannot be estimated from the geochemistry. However, to double the amount of uplift the mountains would have had to have been excessively large. The height of the mountains at the culmination of the Laramide arogeny determines the maximum depth of the basin. The uplift is produced by erosion of the mountains, which removes the load. The lithosphere then comes back up like a leaf spring or a diving board once the diver has jumped. The total amount of uplift is governed by the likely size of the mountains. The high geothermal gradients existed at a considerable distance from the mountains and are not very sensitive to the uncertainty in the size of the load. It is not possible to double the amount of uplift in this region.

D. P. McKenzie. But there are many other causes of uplift besides flexural unloading. Central Africa has certainly not been uplifted by this mechanism. Why has this area not been uplifted by similar epeirogenic movements?

C. Beaumont. The present geothermal gradient on the eastern flank of the basin is now about 55 °C km^{-1}, which is not a great amount less than the 70 °C km^{-1} that we found from the model. Furthermore the water circulation may have been more vigorous when the mountains were higher. So I do not agree that a gradient of 70 °C km^{-1} is excessive. I suspect that similar high gradients exist today on the southern flanks of the Ganga basin in India, the same type of basin. We should see if this is true.

PHILOSOPHICAL TRANSACTIONS OF THE ROYAL SOCIETY A MATHEMATICAL, PHYSICAL & ENGINEERING SCIENCES